Journal of Banking and Finance 145 (2022) 106669

Contents lists available at ScienceDirect

Journal of Banking and Finance

journal homepage: www.elsevier.com/locate/jbf

Expected and Unexpected Jumps in the Overnight Rate: Consistent Management of the Libor Transition☆

Alex Backwell[a,*], Joshua Hayes[a,b]

[a] African Institute of Financial Markets and Risk Management, University of Cape Town, Rondebosch, Cape Town, 7700, South Africa
[b] Fairtree Capital, Newlands, Cape Town, 7700, South Africa

ARTICLE INFO

Article history:
Received 23 March 2022
Accepted 3 September 2022
Available online 7 September 2022

JEL classification:
C63
E43
G12
G13

Keywords:
Benchmark reform
Libor transition
interest-rate jumps
short-rate modelling
stochastic discontinuities
interest-rate options

ABSTRACT

Interest-rate benchmark reform has revived short-rate modelling. One reason is that short-rate models provide a consistent framework in which different benchmarks, and contracts linked to them, can be compared. Another reason is that new benchmarks can be directly dependent on very short-term rates; the key example is a backward-looking compounding of overnight rates, a prominent alternative to forward-looking Libor. Indeed, under Libor, one can often safely ignore aspects of short-rate behaviour, especially jumps. At least partially for this reason, jumps are inadequately treated in the interest-rate literature, particularly expected jumps (jumps with known timing). We estimate a model with expected and unexpected jumps, which involves separating their effect on term rates. We then price forward- and backward-looking caplets, quantifying the spread exhibited by the latter over the former. Expected jumps lead to significantly time-inhomogeneous option behaviour, particularly for short-term options linked to a backward-looking benchmark.

© 2022 Elsevier B.V. All rights reserved.

1. Introduction

We introduce and implement a short-rate modelling framework driven by *expected* and *unexpected* jumps, i.e., jumps with deterministic and stochastic arrival times, respectively. This enables a rigorous comparison of the various interest-rate benchmarks, and associated contracts, involved in the current discussions around the Libor transition. We show that expected jumps have a significant time-inhomogeneous effect on caplets written on backward-looking benchmarks. Although not yet liquid, these are set to become standard interest-rate contracts.

Our model is motivated by Sonia, the major benchmark in the overnight Sterling market; its 2016-2020 time series is shown in the upper panel of Fig. 1. Virtually all variation over the five-year period is driven by four particular jump events.[1] The first three relate to announcements made by the Bank of England's Monetary Policy Committee (MPC), which convenes each quarter to potentially adjust the Bank Rate, which is paid to reserves held at the Bank of England (non-zero adjustments were made once in 2016, 2017 and 2018). The fourth jump is a result of special actions taken by the MPC in March 2020, in response to the COVID-19 pandemic. Fig. 1 also shows two major Sterling term rates that, as we elaborate below, have a clear dependence on the underlying jumps.

Benchmark reform—the transition of major reference rates from Libor-style rates to some alternative—has received significant attention in the academic literature.[2] A renewed interest in short-rate models has resulted, because short rates, given their fine-grained and fundamental nature, can be used to construct different benchmarks, such as a backward-looking compounding of overnight rates, as well as a traditional forward-looking term rate like Libor. One can then examine not only their differing behaviour,

☆ We thank David Skovmand, Obeid Mahomed, and Erik Schlögl for insightful discussions and comments. We also thank two anonymous referees for their comments and suggestions.

* Corresponding author.
E-mail address: alex.backwell@uct.ac.za (A. Backwell).

[1] This kind of behaviour, with a majority of variance being injected at a small set of discrete times, is not rare; other examples can be found in the Eurozone (e.g., Eonia), the US (e.g., Effective Federal Funds) and in emerging markets (e.g., Sabor in South Africa), although the role of spikes, explained further below, may be more prominent.

[2] Prime examples are Lyashenko and Mercurio (2019), Schrimpf and Sushko (2019), Piterbarg (2020) and Klingler and Syrstad (2021). We refer to these papers for discussions of motivations and challenges around the transition. Andersen and Bang (2020) and Gellert and Schlögl (2021) are examples of short-rate modelling motivated by the transition.

https://doi.org/10.1016/j.jbankfin.2022.106669
0378-4266/© 2022 Elsevier B.V. All rights reserved.

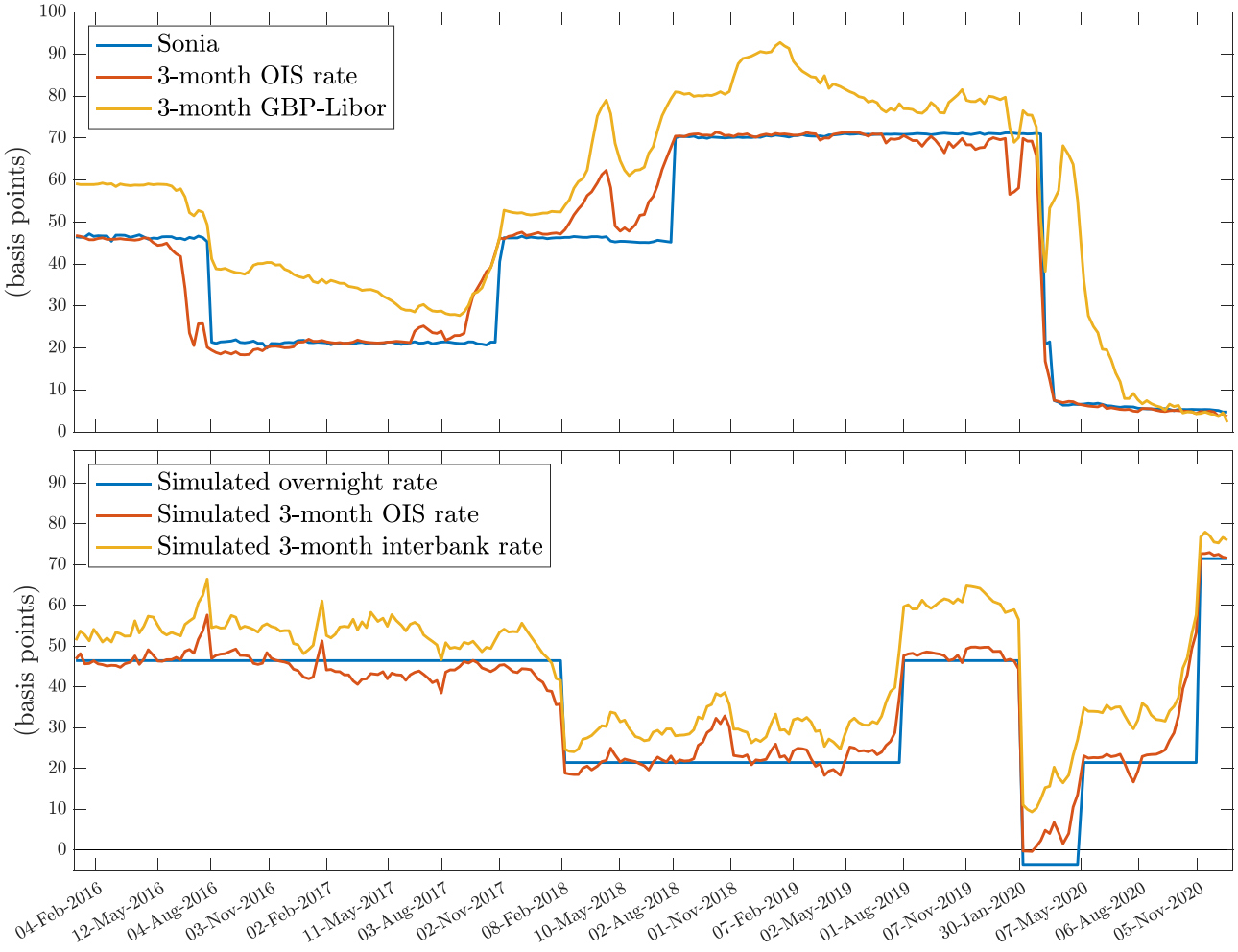

Fig. 1. A comparison of key Sterling-market (upper panel) and model-simulated (lower panel) interest rates. MPC meeting dates are marked on the horizontal axes.

but also that of contracts linked to these new benchmarks, in a consistent and arbitrage-free framework. One can do so in a way that accounts for jumps, and the differing ways that jumps affect different benchmarks (e.g., Libor tends to anticipate a jump, whilst a realised jump enters a back-compounded benchmark directly). Further, a short-rate model that accounts for the varying spread between Libor and overnight-index swap (OIS) rates, thus implying multiple curves, is essential if the potential benchmarks are to be properly handled.[3]

Short-rate variation in our model is driven by expected jumps (sometimes known as stochastic discontinuities, reflecting how the jump size is not known in advance, although the timing is) and also by unexpected jumps (where both the jump time and jump size are not known until they occur). The quarterly meetings of the MPC are a quintessential source of expected jumps. A jump is not guaranteed, but the possibility of a non-zero jump is key to explaining or setting term rates. In the upper panel of Fig. 1, one can see three-month rates anticipate an upcoming MPC meeting, including speculation on the size of the jump before it arrives (we introduce an auxiliary state variable to model this). Some money-market developments are not anticipated, however, such as the pandemic-related rate cut mentioned above. We show that the possibility of such unexpected jumps is also important for explaining term rates.[4] Finally, we model the possibility that an entity's idiosyncratic borrowing cost increases relative to the market (itself subject to expected and unexpected jumps). This possibility is priced into interbank rates, leading to a Libor-OIS spread and multiple curves.[5]

The lower panel of Fig. 1 shows overnight and term rates simulated from our model, with parameters obtained from our empirical estimation. The resemblance of the upper and lower panels (the time-series performance of the model) is a key accompaniment to the close fit we obtain to Sterling OIS and Libor (the cross-sectional performance of the model), with a mean absolute

[3] The term 'multiple curves' refers to the various curves one obtains from stripping swaps with various underling tenors (e.g., three versus six months), when the reference rates are different from the discount rates. This phenomenon was first documented in Henrard (2007).

[4] Formally, we reject the simpler nested model that only includes expected jumps, by comparing the obtained pricing errors; in particular, we obtain an extreme Newey and West (1987) t-statistic based on the hypothesis that unexpected jumps does not improve cross-sectional fit. Informally, OIS rates that do not have an MPC meeting during their term (e.g., the three-month rate immediately after a meeting) are not necessarily equal to Sonia, suggesting a source of variation outside of these meetings.

[5] This approach to multi-curve modelling was introduced by Filipović and Trolle (2013) and refined by Alfeus et al. (2020), who term this possibility *downgrade risk*, or, more generally, *rollover risk*. We focus on the Libor-OIS spread, but as an example of the multi-curve nature of our model, note that model-fitted six-month Libor averages 65 basis points over our sample, while the average (simply compounded) six-month rate bootstrapped from three-month Libor and the '3x6' Libor-linked forward rate agreement (both model-fitted) is 53 basis points. Thus, the six-month point on the 'three-month curve' differs from that on the 'six-month curve'.

fitting error of about one basis point. An important background aspect of our estimation is the separation of the effects of expected and unexpected jumps on term rates; the time-inhomogeneous effect of expected jumps allows the pricing equation at any particular cross section to be inverted. Expected jumps turn out to be responsible for about half of the magnitude of OIS-Sonia spreads, but for around 80% of their variability. Informed by this, we can calculate risk-adjusted expectations of future short rates, allowing different benchmarks and associated contracts to be handled. We calculate premia for forward-looking caplets (linked to a traditional interbank rate) and for backward-looking caplets (linked to a compounding of Sonia); we do this over our 2016-2020 sample period, accounting for whether and precisely where a jump is expected during the reference rate's accrual period, and for how unexpected jumps are priced into term rates at the time. Forward-looking options can disguise the time-inhomogeneity of expected jumps (because standardised times-to-expiry tend to ensure that a constant number of jumps are expected during the option's life), unlike backward-looking options (which depend on the timing of the jumps during the compounding period). We quantify the spread that backward-looking caplets exhibit over traditional Libor caplets, which can be seen as a Jensen gap, finding it to be significant and also significantly time inhomogeneous, with option premia dropping by as much as 30% as an expected jump leaves the relevant time frame. Especially for short-term options, one should not naively convert the implied volatility of one type of caplet to another. At-the-money strikes (and, more generally, option moneyness) can change significantly under different benchmarks; we show the changes in option value to be significant if this is not carefully managed.

Now consider our paper in the context of the literature.[6] Fontana et al. (2020) highlight two key features of modern interest-rate markets: expected jumps and multiple curves, both of which are included in our model. Their study is mathematical; ours is applied. They use a generalised Heath et al. (1992) (HJM) framework to capture and analyse a broad class of term structure models with the two key features. In their model, Fontana et al. (2020) distinguish between 'type I' and 'type II' jumps, which we shall call *jumps* and *spikes*, respectively. Although not prominent in the Sterling market, spikes—where the short rate jumps and then rapidly returns to the pre-jump level—can have a significant presence, often resulting from certain liquidity pressures that arise at the end of reporting periods.[7,8] The focus of the present paper is on jumps with a persistent effect, and not on spikes; though we do discuss the addition of a spike component to our model in Appendix D, and view this aspect of the literature as complementary to our approach.

Fontana et al. (2020) note the absence of interest-rate models with expected jumps; indeed, with the exception of Gellert and Schlögl (2021), existing models are not able to satisfy both the time-series and cross-sectional comparisons mentioned above.[9] Gellert and Schlögl (2021) focus on the Secured Overnight Financing Rate (SOFR), which is central in the benchmark-reform discussion in the USA. They fit into the framework of Fontana et al. (2020), focusing on spikes, a prominent feature of SOFR, and also expected jumps. In common with us, a key feature of their model is the piecewise constant, jump-driven short rate, along with diffusively evolving term rates. Their jumps arise from switching on an accumulated increment of Brownian motion, whereas we allow for a general jump distribution (and implement a discrete instance akin to Fig. 1, where most jumps are 25 basis points in magnitude). An advantage of our short-rate framework is that term rates are given by a function of the short rate and any auxiliary state variables, in which the system is naturally Markov; the approach of Gellert and Schlögl (2021) is not amenable to state variables that adjust jump distributions (particularly risk-adjusted jump means) over time. Andersen and Bang (2020) consider short-rate models in the context of benchmark reform: their focus is on SOFR, on its spikes, and the different ways the return jumps, or spike decay, can be modelled. They price SOFR-linked caplets, accounting for expected and unexpected spikes.

Babbs and Webber (1994) are an early source on modelling the short rate as an intensity-driven pure-jump process. Interestingly, although they do not consider expected jumps, their model closely resembles ours; an auxiliary state variable is used to model market perceptions of the likely size of future jumps. See Table 1 for a summary of how our paper compares to the existing literature.

Finally, we note that our jump-driven model resolves a contradiction in the short-rate modelling literature: traditional models exhibit mean reversion, and consequently tend to imply decreasing volatility term structures, while market volatility term structures decidedly increase.[10] Specifically, the time-series volatility of lending or swap rates (the standard deviation of rate changes) is larger for longer terms, out to at least a few years.[11] Our model naturally exhibits this feature, with our auxiliary state variables modelling variation in the market's perception of upcoming jumps, resulting in term rate variation. As the term becomes shorter, sensitivity to the auxiliary state variables decreases, as potential jumps have less ability to affect the average rate over the shorter accrual period (at the short-term limit, volatility is zero, unless a jump happens to occur in the measurement period).[12] A common resolution to this contradiction is to introduce negative correlation between state variables controlling the yield curve (see the discussions in Piazzesi (2010, §7.6) and Brigo and Mercurio (2007, Ch.4.1) and the references therein). This can engineer an increasing volatility term structure, because a state variable's effect on short-term rates can be offset by the effect of another negatively correlated state variable, while leaving a net effect on longer term rates.[13] This is unsatisfactory, in our view, because this negative-correlation ap-

[6] Our literature review is not exhaustive, and focuses on a few pertinent papers. The short-rate modelling literature in general is considerable and mature; jumps have been considered for many years, going back to Babbs and Webber (1994), and more recently in, e.g., Jiao et al. (2017). Expected jumps are much more scarce, but go back to Piazzesi (2001), with a more recent treatment in Kim and Wright (2014). To our knowledge, we are the first to treat expected and unexpected jumps together, and are among the first to study the interaction of jumps and benchmark reform (other studies are mentioned in our review).

[7] See Gellert and Schlögl (2021) and Andersen and Bang (2020) for detailed discussions of spikes.

[8] Sonia previously exhibited relatively small but non-negligible spikes prior to a methodology reform which we discuss in Section 3.1. Fig. 1 (and this whole paper) works with a weekly step size, which disguises five minor (roughly five-basis-point) spikes in the earlier part of the sample, each appearing for one reporting day. The effect of such spikes on term rates is very small (e.g., five additional basis points for one day leads to about a one-quarter basis point change in the one-month term rate).

[9] A Brownian-based diffusion model for the short rate could imply a good fit to the data considered in this paper (given a sufficient number of states and parameters), but not a plausible simulation. Skov and Skovmand (2021), for example, show that a traditional affine-diffusion model can cross-sectionally fit SOFR term rates.

[10] Positive mean reversion under a risk-adjusted measure implies that variation in the short rate has an (increasingly) damped effect on (increasingly) longer term rates. In fact, the 'long rate' implied by short-rate models is usually a constant (that it cannot fall is quite well known; see Dybvig et al. (1996)).

[11] Volatility term structures, time-series-based or implied, do tend to decrease eventually, resulting in an overall *humped* shape; see, e.g., Brigo and Mercurio (2007, Ch.3.7).

[12] This logic applies to both the excepted and unexpected jumps in our model, with one specific exception: the moment before an expected jump, rates of all terms are equally sensitive to the jump realisation.

[13] The clearest example is the G2++ model of Brigo and Mercurio (2007, Ch.4.2), with the short rate given as $r_t = x_t + y_t$, where the innovations to x_t and y_t typically have a near-perfect negative correlation. Whatever x_t-innovation is experienced, there tends to be an equal and opposite y_t-innovation, leaving the short rate

Table 1
Summary showing where the present paper sits within the literature.

	expected jumps	unexpected jumps	auxiliary state(s)	multiple curves	spikes
This paper • pure-jump short rate; diffusive term rates • general jump distribution	✓	✓	✓	✓	✗
Fontana et al. (2020) • fully theoretical	✓	✗	✗	✓	✓
Gellert and Schlögl (2021) • pure-jump short rate; diffusive term rates • jumps driven by accumulated Brownian motion	✓	✗	✗	✗	✓
Andersen and Bang (2020) • focus on SOFR-linked caplet pricing	✗	✗	✗	✗	✓
Babbs and Webber (1994) • pure-jump short rate; diffusive term rates	✗	✓	✓	✗	✗

proach does not resemble the mechanism behind market volatility structures, while our model does: changes in the overnight rate are continually anticipated, updated and priced into term rates, with a naturally stronger effect for longer terms. As with the multiple curves, this structure arises endogenously.

Section 2, below, outlines the general framework of models under consideration, as well as a specific instance of this framework. Section 3 presents our empirical implementation of this model instance. Section 4 concludes.

2. Modelling framework

2.1. Short rate specification

Letting r_t denote the time-t short-term risk-free interest rate, consider models of the following form:

$$dr_t = J_t^{\mathrm{e}}\, dN_t^{\mathrm{e}} + J_t^{\mathrm{u}}\, dN_t^{\mathrm{u}}, \tag{1}$$

where N_t^{e} and N_t^{u} are counting processes that model the timing of jumps in the short rate, with J_t^{e} and J_t^{u} being corresponding jump sizes.[14] In particular, N_t^{e} models expected, or deterministically timed, jump events. Therefore, $dN_t^{\mathrm{e}} = \mathbb{I}(t \in \mathcal{T})$, where $\mathcal{T}$ is the set of known jump times. Unexpected jumps, with random times, are modelled by N_t^{u}, which would usually be specified to admit an intensity.[15]

The sizes of jumps in the short rate can be distributed in a way that depends on some auxiliary state process, which we denote x_t. For example, one could specify that $J_s^{\mathrm{e}} \sim N(x_s, \sigma^2)$ for all $s \in \mathcal{T}$, where x_t is some scalar-valued process and σ a constant. More generally, x_t can be vector-valued, and its various components can control the mean, variance, or any other aspect of the distributions of J_t^{e} and J_t^{u}. It is practical for r_t and x_t to be jointly Markov: that is, for the values of these two processes at some time point to be sufficient to characterise their later behaviour.

Sonia, plotted in Fig. 1, is an unsecured rate, and forms the basis of our empirical implementation in Section 3 below. We denote the unsecured, or credit-risky, time-t short rate by

$$r_t^* = r_t + \Lambda_t, \tag{2}$$

where Λ_t denotes the time-t average credit spread in the overnight borrowing market or some sub-market thereof. For our purposes, it is convenient to rewrite the model in terms of the unsecured rate:[16]

$$dr_t^* = J_t^{\mathrm{e}}\, dN_t^{\mathrm{e}} + J_t^{\mathrm{u}}\, dN_t^{\mathrm{u}}. \tag{3}$$

Nor is generality lost in assuming zero recovery in the event of default, allowing us to identify Λ_t as the instantaneous default intensity associated with the time-t market.[17]

While we shall focus on the implications of expected and unexpected jumps, one could consider adding other aspects to the specifications (1) or (3), e.g., terms that produce spikes or continuous, Brownian variation. In Appendix D, we briefly consider the former, and show how our non-spiking model fares in the presence of spikes of various magnitudes.

2.2. Derived term rates

With the short rate in place, consider now term instruments, such as a swap or a three-month loan. Risk-adjusted expectations of the short rate (and perhaps credit-worthiness) during the term in question are the key consideration in setting term rates. To ensure these risk adjustments are consistently implemented in our model, we assume the existence of a risk-adjusted probability measure, denoted $\mathbb{Q}$, equivalent to the physical measure, $\mathbb{P}$. Under $\mathbb{Q}$, any investable, self-financing process is a martingale after discounting with the short rate. Arbitrage is thus excluded from the model.[18] Even in the absence of capital constraints, trading costs and other frictions, one cannot make profits without taking on some cost or some risk; more generally, expected returns above the short rate can only be earned by bearing risk, in line with the market-determined price of risk.

We defer the technical details around the measure change to Appendix A.1. In short, one needs to specify jumps K_t^{e} and K_t^{u}, corresponding to J_t^{e} and J_t^{u}, which leads to a Radon-Nikodym deriva-

unchanged, but having an effect on term rates (because of different decay rates of the two innovations).

[14] All probability-theoretic notions in the paper are defined in the context of a filtered probability space $(\Omega, \mathcal{F}, \{\mathcal{F}_t\}, \mathbb{P})$.

[15] I.e., one would ensure that $\lim_{\delta \downarrow 0} \frac{1}{\delta} \mathbb{P}(N_{t+\delta}^{\mathrm{u}} > N_t^{\mathrm{u}} \mid \mathcal{F}_t)$ exists.

[16] In principle, (1) should now be amended to include term $d\Lambda_t$. However, it will become clear that, for our purposes, separate modelling of r_t and Λ_t is not required or relevant; our applications depend only on the sum r_t^* and the specification (2). This is because we do not work with any data that depends on default separately from how it is reflected in credit spreads (such as credit default swap spreads, or observations of default events). See Filipović and Trolle (2013) and Backwell et al. (2019) for studies that work with credit default swaps and discuss this issue in detail.

[17] The fact that default intensity and credit spread coincide in the absence of recovery is well known; see, e.g., Filipovic (2009, Ch.12). If one assumed that some non-zero fraction of pre-default market-value is recovered, as per Duffie and Singleton (1999), all of our results would be recovered. Greater intensities would be needed to match market credit spreads, but nothing would change besides this rescaling. There would be a minor approximation if other recovery assumptions, e.g. recovery of par, were applied.

[18] Existence of a risk-adjusted measure is well known to be a sufficient condition to preclude arbitrage in the standard sense of risk-free cost-free profit opportunities. The existence of a risk-neutral measure is necessary to avoid the stronger condition of no free lunch with vanishing risk. See, e.g., Björk (2004, Ch.10).

tive that formally characterises $\mathbb{Q}$. These market-price-of-risk processes control how the physical-measure distribution of J_t^i differs from its risk-adjusted counterpart. Also, K_t^{u} controls the relationship between the physical and risk-adjusted jump intensities of N_t^{u}.[19]

Consider first a risk-free term loan (e.g., a fully collateralised loan). We define and denote the time-t risk-free discount factor, for an accrual period ending at time $T \geq t$, with

$$P_{tT} = \mathbb{E}_t\left[e^{-\int_t^T r_u du}\right], \tag{4}$$

where $\mathbb{E}_t[\cdot]$ denotes time-t conditional expectation under $\mathbb{Q}$. One can lend an amount P_{tT} at time t in order to receive one unit at T. Scaling this, one can lend one unit at t to receive, at T,

$$\frac{1}{P_{tT}} = 1 + R_{tT}(T-t), \tag{5}$$

where R_{tT} denotes the simple term rate over the period $[t, T]$.[20]

To capture an unsecured loan in the context of an interbank market, consider the following variation of the risk-free bond price (4):

$$P_{tT}^L = \mathbb{E}_t\left[e^{-\int_t^T r_u du}\mathbb{I}(\tau^{(t)} > T)\right], \tag{6}$$

where the indicator $\mathbb{I}(\cdot)$ explicitly models a zero-recovery default, with $\tau^{(t)}$ denoting the default time of an average but specific entity from the time-t market in question, e.g., the Libor panel. The inevitable fixing of a specific borrower introduces the possibility of a departure from the market average; while market interest rates and credit spreads can rise, so can the borrower's default intensity and fair credit spread *relative to the market*; this can be called downgrade risk or roll-over risk.[21]

With a minor abuse of conditional-expectation notation, one can simplify (6) to[22]

$$\begin{aligned} P_{tT}^L &= \mathbb{E}_t\left[e^{-\int_t^T r_u du}e^{-\int_t^T (\Lambda_u + \lambda_u^{(t)})du}\right] \\ &= \mathbb{E}_t\left[e^{-\int_t^T (r_u^* + \lambda_u^{(t)})du}\right], \end{aligned} \tag{7}$$

where $\lambda_u^{(t)}$ denotes the time-u default intensity of an entity fixed at time t *relative to the market average*. That is, the entity has a time-u default intensity of $\Lambda_u + \lambda_u^{(t)}$, and, because Libor pertains to an average bank (at the time of fixing), one has that

$$\lambda_t^{(t)} = 0 \tag{8}$$

for all $t \geq 0$. After the loan fixing time t, the borrower can depart from the market average; the borrower could upgrade, meaning their default intensity is lower than the market average Λ_u, so that $\lambda_u^{(t)} < 0$, or the borrower could downgrade, with $\lambda_u^{(t)} > 0$. Downgrades are not guaranteed, but their possibility tends to be priced into the term rates of credit-risky loans. While upgrades may be possible, note that the total intensity, $\Lambda_u + \lambda_u^{(t)}$, must remain non-negative.

Because we are considering initially average entities, (8) must always initiate the downgrade process, for any initiation time t_0 at which the borrower is fixed. As in Section 2.1, it is practical for the family of downgrade processes to be Markov with respect to the state process x_t, so that (7) can be given as a function of r_t^* and x_t.

As per (5), define the simple interbank rate L_{tT} via

$$\frac{1}{P_{tT}^L} = 1 + L_{tT}(T-t). \tag{9}$$

Collateralised contracts and associated cash flows must of course be handled differently. Consider an overnight-index swap (OIS), where an overnight rate is compounded to form a floating rate that is swapped for a fixed rate. Typically, OISs i) are linked to an unsecured overnight rate; ii) are themselves fully collateralised with a dynamically maintained margin account; and iii) pay interest on collateral accounts in line with the unsecured overnight rate. Assuming i), the net long payoff of an OIS running from t to $T > t$ becomes

$$e^{\int_t^T r_u^* du} - 1 - \mathrm{OIS}_{tT}(T-t), \tag{10}$$

where we approximate daily compounding with the continuous limit.[23,24] In addition to OIS contracts, there is an active futures market linked to Sonia. Like an OIS, these contracts depend linearly on compounded Sonia; the key difference is the convexity adjustment associated with futures (see Skov and Skovmand (2021)).

Discounting (10) at the collateral rate, due to ii) and iii), one finds a variation of (9):[25]

$$\frac{1}{P_{tT}^*} = 1 + \mathrm{OIS}_{tT}(T-t), \tag{11}$$

where

$$P_{tT}^* = \mathbb{E}_t\left[e^{-\int_t^T r_u^* du}\right]. \tag{12}$$

Comparing (7) and (12), one can see how the Libor-OIS spread is driven by the downgrade process $\lambda_u^{(t)}$, while the (unsecured) short-rate process drives OIS rates.[26] An attractive feature of this approach is that the term structure of Libor-OIS spreads, and therefore the relationship between the 'multiple curves' that arise from instruments referring to different Libor terms, becomes an endogenous property.[27]

The floating OIS payment, based on overnight-compounding, has attracted much attention in the discussions around benchmark reform. Expressing this as an annualised rate, define

$$B_{tT} = \left(e^{\int_t^T r_u^* du} - 1\right)/(T-t). \tag{13}$$

[19] See Appendix A.1. The market awards a risk premium to both the timing and the size aspects of the unexpected jumps; the risk-adjusted jump intensity is given by the physical intensity multiplied by $1 + \bar{\mathbb{E}}_t[K_t^{\mathrm{u}}]$, where $\bar{\mathbb{E}}_t[\cdot]$ denotes conditional physical-measure expectation, immediately before an unexpected jump is realised. With $\mathbb{P}$ and $\mathbb{Q}$ being equivalent, the known timing of the expected jumps must remain under both measures.

[20] We ignore day count adjustments throughout the paper.

[21] See Filipović and Trolle (2013) and Alfeus et al. (2020) for thorough treatments of this concept. In a term loan, the borrower passes downgrade (or roll-over) risk to the lender, just as interest-rate risk is borne by the lender; that is, a borrower can avoid roll-over risk by borrowing at term rather than on a rolling basis. Roll-over risk can encompass more than a credit downgrade; non-credit increases in borrowing costs relative to the market have proved to be significant as well.

[22] The notation does not reflect that these conditional expectations are based on a smaller sigma-algebra than in (6); in particular, they are based on $\mathcal{F}_t^1$, where $\mathcal{F}_t = \mathcal{F}_t^1 \vee \mathcal{F}_t^2$, with $\{\mathcal{F}_t^2\}$ generated by the default indicators $\mathbb{I}(\tau^{(t)} > T)$. See, e.g., Filipovic (2009, Ch. 12). One would often see an indicator $\mathbb{I}(\tau^{(t)} > t)$ appearing outside of these expectations, but we straightforwardly have $\mathbb{I}(\tau^{(t)} > t) = 1$, having defined $\tau^{(t)}$ as the default time of an average (and therefore non-defaulted) time-t entity.

[23] I.e., $e^{\int_t^T r_u^* du} \approx \prod_{i=0}^{n-1}(1 + r_{t_i}^*(t_{i+1} - t_i))$, where $t = t_0 < t_1 < \ldots < t_n = T$. This is a common approximation (see, e.g. Filipović and Trolle (2013, §2.5)) and we make it throughout the paper.

[24] We have considered single-period OISs only, which is conventional provided the maturity is one year or less. If the maturity is larger, periodic payments are made and (10) would need to be generalised. See, e.g., Alfeus et al. (2020, §2.3).

[25] See Filipović and Trolle (2013, §2.2) for discussion of collateralised-contract pricing.

[26] Because our study is based on an unsecured rate, Sonia, market-average credit risk (modelled with Λ_t) is bundled together with interest rate risk (modelled by r_t). As alluded in Section 2.1, a secured overnight reference rate could be accommodated by straightforward changes in our framework. In that case, Libor-OIS spreads would be driven by total (both market and idiosyncratic) credit risk $\Lambda_u + \lambda_u^{(t)}$.

[27] In contrast, multiple-curve models often model each curve, corresponding to each reference term, with separate, ad-hoc spreads (without structural links between the curves, or any account of how the spreads arise); see Alfeus et al. (2020) for a detailed discussion.

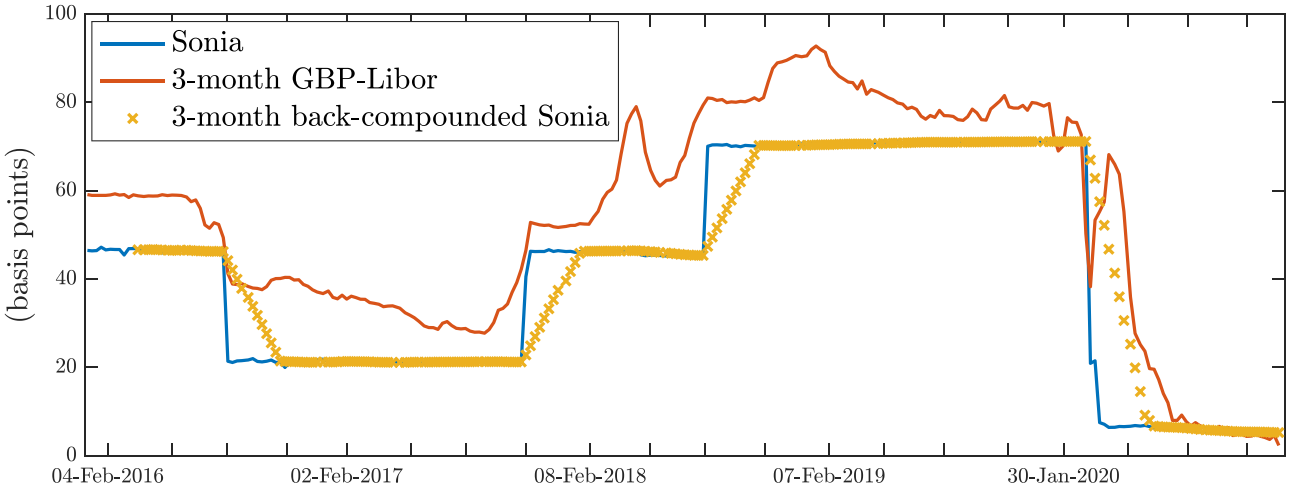

Fig. 2. A comparison of different benchmark rates in the Sterling market. MPC meeting dates are marked on the horizontal axis, but the specific dates are suppressed aside from the first each year.

Like the OIS rate in (11) but unlike the interbank rate in (9), credit risk appears in an overnight sense only; the rate is free from the downgrade risk that arises from a fixed borrower. Unlike the rates in (9) and (11), (13) is backward-looking, in that it is observable no earlier than T, the end of the accrual period; mathematically, it lacks the time-t conditional expectation appearing in a forward-looking alternative.

These effects can be seen in Fig. 2, which compares the realised time series of three-month interbank rates, corresponding to $L_{t,t+0.25}$, and rates from a three-month backward compounding of overnight Sonia, corresponding to $B_{t,t+0.25}$. Firstly, the Sonia-Libor spread is significant (affecting, e.g., the setting of at-the-money strike rates; see Section 3.5 below), giving downgrade risk an important role in our modelling framework. Secondly, $B_{t,t+0.25}$, by its back-compounded nature, responds to jumps only after they are realised, unlike forward-looking $L_{t,t+0.25}$, which often incorporates views about the likely size of the jump from up to three months in advance. The details of a particular contract—its maturity and whether it refers to a backward- or forward-looking rate—can change whether and how the contract is exposed to a specific expected jump. As discussed in Section 1, short-rate models like those in this section provide a consistent framework in which one can consider and compare forward-looking L_{tT}, backward-looking B_{tT} and contracts linked to either.

2.3. Model instance

We now specify an instance of the modelling framework outlined above, with the goal of capturing the data in Fig. 1. The expected jumps in (3) occur quarterly, as per the MPC meeting schedule discussed in Section 1, while the unexpected jumps dN^{u}_t arrive at a constant risk-adjusted intensity denoted ν^{u} (independently of other aspects of the model). We model downgrade risk with unexpected jumps in creditworthiness; for all $t_0 \geq 0$,[28]

$$d\lambda^{(t_0)}_t = \max(J^{\mathrm{d}}_t, -\Lambda_t)\, dN^{\mathrm{d}}_t, \qquad \lambda^{(t_0)}_{t_0} = 0, \tag{14}$$

where N^{d}_t is a counting process modelling the times at which some entity's credit spread changes relative to the market, with J^{d}_t representing the size of such changes. These times arrive at a constant risk-adjusted intensity denoted ν^{d} (again independently). We specify a distribution for J^{d}_t below, but the max operator in (14) ensures that, for any distribution, the total default intensity $\Lambda_t + \lambda^{(t_0)}_t$ remains non-negative. We set Λ_t to twenty-five basis points (bps).[29]

We work with a three-dimensional auxiliary state process, with scalar components corresponding to expected and unexpected short-rate jumps, and credit-downgrade jumps, respectively: $x_t = [x^{\mathrm{e}}_t\ x^{\mathrm{u}}_t\ x^{\mathrm{d}}_t]^\top$. Before we specify dynamics for x_t, we explain how its value controls the jump distributions. Intuitively, x^i_t represents the time-t (risk-adjusted) market-aggregate view about the likely size of the upcoming jump (whether in the case of expected or unexpected short-rate jumps, or credit-downgrade jumps, i.e., $i \in \{\mathrm{e}, \mathrm{u}, \mathrm{d}\}$). Specifically, we consider discrete distributions for J^i_t, with five jump possibilities, symmetric around zero, with gaps of twenty-five bps. This is motivated by the Sonia time series plotted above, where the first three jumps have a magnitude of twenty-five bps, and the final (pandemic-related) jump was initially fifty bps (negative), followed by a further fifteen bps. Consider initially the situation where $x^i_t = 0$, representing a market that is neutral about the upcoming jump. Neutral here means the risk-adjusted expectation of the jump is zero, and therefore no premium is necessary to protect lenders from the upcoming jump.[30] The probability of no jump, $J^i_t = 0$, is given by parameter p^i_*, with the remaining probability, $1 - p^i_*$, equally distributed over the four possibilities, $J^i_t \in \{-50\text{bps}, -25\text{bps}, 25\text{bps}, 50\text{bps}\}$. This gives p^i_* control over jump variance, with $p^i_* = 0$ and $p^i_* = 1$ implying maximum and minimum variance, respectively; Section 3.2 below discusses this further.

If x^i_t becomes positive, then probability is shifted (in a way that we formalise shortly) from the negative side to the positive side of the distribution. This increases the mean of the distribution without shifting the fixed discrete support ranging from negative to positive fifty bps. The effect of negative x^i_t is symmetric, shifting probability to the negative jump possibilities. Formally, for $i = \mathrm{e}, \mathrm{u},$

[28] This specifies a *family* of downgrade processes, indexed by the initial fixing time $t_0 \geq 0$, for each of which there is a downgrade process $\lambda^{(t_0)}_t$ (for $t \geq t_0$). Strictly speaking, J^{d}_t and N^{d}_t should be similarly indexed, as different initial borrowers will realise different downgrades; we avoid this notational burden, however, as only the marginal distribution of each downgrade process is relevant to (7).

[29] See Backwell et al. (2019), who show that the market credit spread is higher than previously supposed. Recalling that this paper depends on the unsecured rate r^*_t but not its decomposition (see Footnote 26), we note that the specification of Λ_t has very little effect on our implementation; none, in fact, beside the truncation in (14).

[30] If, however, x^i_t is expected to be non-zero during the life of a loan, a term premium can prevail.

Table 2
An elaboration on the jump distributions specified in (15).

	$\mathbb{Q}(J_t^i = j \mid x_{t^-}^i = x)$		
	$j = -50$bps, -25bps	$j = 0$	$j = 25$bps, 50bps
$\lvert x\rvert \le \frac{1}{2}(1 - p_*^i)$	$\frac{1}{4}(1 - p_*^i) - \frac{1}{2}x$	p_*^i	$\frac{1}{4}(1 - p_*^i) + \frac{1}{2}x$
$x \in \left(\frac{1}{2}(1 - p_*^i), \frac{1}{2}\right)$	0	$1 - 2x$	x
$x \ge \frac{1}{2}$	0	0	$\frac{1}{2}$
$x \in \left(-\frac{1}{2}, -\frac{1}{2}(1 - p_*^i)\right)$	$-x$	$1 + 2x$	0
$x \le -\frac{1}{2}$	$\frac{1}{2}$	0	0

and d,

$$\mathbb{Q}(J_t^i = j \mid x_{t^-}^i = x) = \begin{cases} \min\left(\frac{1}{2}, \max\left(0, \frac{1}{4}(1 - p_*^i) - \frac{1}{2}x, -x\right)\right) & \text{if } j = -50\text{bps}, -25\text{bps}; \\ \max\left(0, \min(1 - 2x, 1 + 2x, p_*^i)\right) & \text{if } j = 0; \\ \min\left(\frac{1}{2}, \max\left(0, \frac{1}{4}(1 - p_*^i) + \frac{1}{2}x, x\right)\right) & \text{if } j = 25\text{bps}, 50\text{bps}. \end{cases} \tag{15}$$

For reasons that will shortly become clear, the distribution of time-t jump depends on the auxiliary state value immediately before t (i.e., the left limit $x_{t^-}^i$). This distribution is made more explicit in Table 2, where the various ranges of $x_{t^-}^i$ are considered. Provided that $x_{t^-}^i$ is not overly positive or negative (i.e., $|x_{t^-}^i| \le \frac{1}{2}(1 - p_*^i)$), the first row shows how probabilities shift between the positive and negative jump possibilities. When $|x_{t^-}^i| = \frac{1}{2}(1 - p_*^i)$, probability on one side of the distribution runs out, and must be taken from the zero-jump possibility if $|x_{t^-}^i| > \frac{1}{2}(1 - p_*^i)$. The specification (15) ensures that the probabilities, and therefore the mean, change continuously in x_t^i, resulting in

$$\mathbb{E}_{t^-}[J_t^i] = \begin{cases} -37.5\text{bps} & \text{if } x_{t^-}^i < -\frac{1}{2}, \\ 75 x_{t^-}^i\text{bps} & \text{if } |x_{t^-}^i| \le \frac{1}{2}, \\ 37.5\text{bps} & \text{if } x_{t^-}^i > \frac{1}{2}. \end{cases} \tag{16}$$

When $|x_{t^-}^i| = \frac{1}{2}$, all of the probability has been shifted to the non-zero jumps on one side of the distribution, limiting how far the mean can be moved from zero.

While our general framework begins under the physical measure, and then changes to the risk-adjusted measure, it can be more convenient to go in the opposition direction. We require that x_t satisfies

$$dx_t^{\mathrm{e}} = \left(\sigma^{\mathrm{e}} + \beta^{\mathrm{e}} |x_t^{\mathrm{e}}|\right) dW_t^{\mathrm{e}}, \qquad x_s^{\mathrm{e}} = 0 \text{ for all } s \in \mathcal{T}, \tag{17}$$

$$dx_t^{\mathrm{u}} = \kappa^{\mathrm{u}}(\theta^{\mathrm{u}} - x_t^{\mathrm{u}})\, dt + \sigma^{\mathrm{u}}\, dW_t^{\mathrm{u}}, \tag{18}$$

$$dx_t^{\mathrm{d}} = \kappa^{\mathrm{d}}(\theta^{\mathrm{d}} - x_t^{\mathrm{d}})\, dt + \sigma^{\mathrm{d}}\, dW_t^{\mathrm{d}}, \tag{19}$$

where $[W_t^{\mathrm{e}}\ W_t^{\mathrm{u}}\ W_t^{\mathrm{d}}]^\top$ is a three-dimensional standard (independent) Brownian motion under risk-adjusted $\mathbb{Q}$. The Ornstein-Uhlenbeck dynamics in (18) and (19) model the fluctuation of the market view about unexpected jumps. The mean reversion rates κ^{u} and κ^{d} control how the effect of this view is distributed over the term structure.[31]

The latter part of (17) ensures that x_t^{e} *resets* after each quarterly jump time (stored in $\mathcal{T}$). Because of this reset, x_t^{e} should be interpreted as conveying market views about the next expected jump, but not any jumps after that. The value immediately before a jump and reset (i.e., $x_{s^-}^{\mathrm{e}}$ for $s \in \mathcal{T}$) determines the distribution of J_s^{e}, as per (15) above. Besides these resets, x_t is continuous, so that $x_{s^-}^{\mathrm{e}} = x_s^{\mathrm{e}}$ for $s \notin \mathcal{T}$, and $x_{s^-}^{\mathrm{u}} = x_s^{\mathrm{u}}$ and $x_{s^-}^{\mathrm{d}} = x_s^{\mathrm{d}}$ for all $s \ge 0$. The dynamics in (17) do not feature mean reversion, because the effect of x_t^{e} on the term structure is already naturally controlled by the timing of the next expected jump. For example, if the next expected jump is in one month, terms of one month or less are not affected by the current value of x_t^{e}, but terms greater than one month are increasingly sensitive to x_t^{e}.[32] The parameter β^{e} gives x_t^{e} *self-exciting* volatility dynamics, where any departure from the reset value zero results in greater volatility. This is motivated by the patterns in Fig. 1, where expectations regarding an upcoming jump are *occasionally* priced into term rates, but most quarterly jumps are not accounted for.

While the measure-change formalities are deferred to Appendix A.1, the adjustment of the dynamics to these Brownian-driven processes is well known to be of the following form:

$$dx_t^{\mathrm{e}} = \left(\sigma^{\mathrm{e}} + \beta^{\mathrm{e}} |x_t^{\mathrm{e}}|\right)\left(d\bar{W}_t^{\mathrm{e}} - \mu_t^{\mathrm{e}}\, dt\right) \tag{20}$$

$$dx_t^{\mathrm{u}} = \kappa^{\mathrm{u}}(\theta^{\mathrm{u}} - x_t^{\mathrm{u}})\, dt + \sigma^{\mathrm{u}}\left(d\bar{W}_t^{\mathrm{u}} - \mu_t^{\mathrm{u}}\, dt\right) \tag{21}$$

$$dx_t^{\mathrm{d}} = \kappa^{\mathrm{d}}(\theta^{\mathrm{d}} - x_t^{\mathrm{d}})\, dt + \sigma^{\mathrm{d}}\left(d\bar{W}_t^{\mathrm{d}} - \mu_t^{\mathrm{d}}\, dt\right), \tag{22}$$

where $[\bar{W}_t^{\mathrm{e}}\ \bar{W}_t^{\mathrm{u}}\ \bar{W}_t^{\mathrm{d}}]^\top$ is a three-dimensional standard Brownian motion under the physical measure $\mathbb{P}$, and $[\mu_t^{\mathrm{e}}\ \mu_t^{\mathrm{u}}\ \mu_t^{\mathrm{d}}]^\top$ is a corresponding market-price-of-risk process, which we set as constant, with individual scalars μ^{e}, μ^{u} and μ^{d}. This completes the specification of the three-dimensional auxiliary state process x_t, the first two components of which control the distribution of expected (quarterly) and unexpected jumps in the unsecured short rate, with the final component similarly controlling unexpected credit downgrades.

Our model generalises that of Babbs and Webber (1994); they specify a short-rate process driven by unexpected jumps (but not expected jumps), and, like us, a Brownian-driven auxiliary state variable that controls the jump distribution. They do not specify a jump distribution, but explain how their state variable should be allowed to dictate the relative likelihood of various jump sizes.[33] Our model with unexpected jumsps only (and no expected jumps or downgrade risk) is thus an implementation of the Babbs and Webber (1994) framework.

[31] A large positive κ^{u}, for example, will limit the effect of x_t^{u} on longer term loans.

[32] The moment before an expected jump is the only time that the whole term structure is equally exposed to the jump and therefore to x_t^{e}. The changing sensitivities over time (in other words, the time inhomogeneity of the pricing function that will result from (4)) is important in the background workings of the filter we use in Section 4, where the x_t^{e} and x_t^{u} must be separately identified.

[33] Instead of explicitly discussing a distribution for jump size, Babbs and Webber (1994) have different Poisson processes corresponding to each potential jump size, with the auxiliary state controlling the competing jump intensities, leading to an implicit distribution.

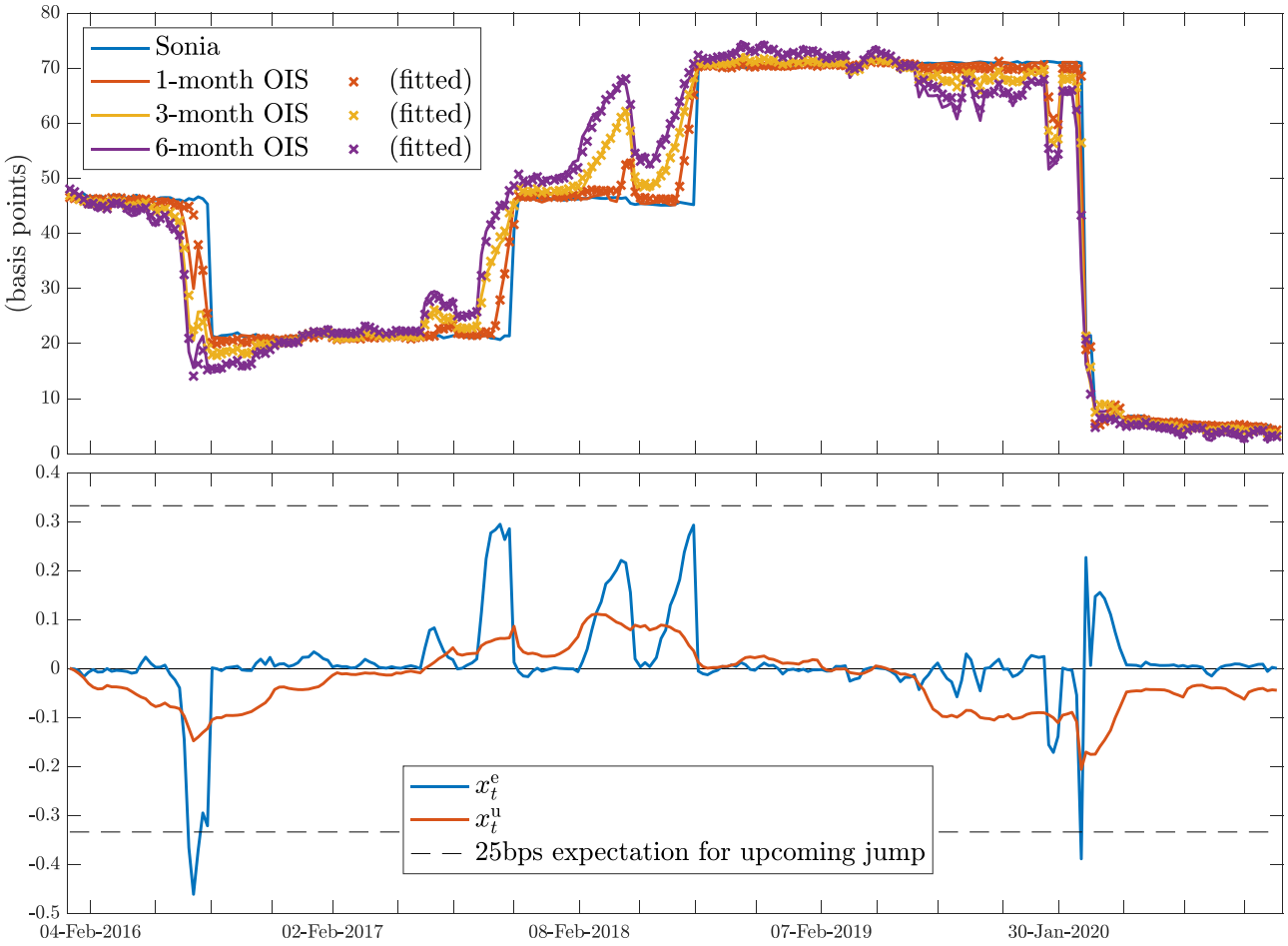

Fig. 3. A comparison of market and model-fitted OIS rates in the upper panel; filtered state variable paths in the lower panel. MPC meeting dates are marked on the horizontal axes.

3. Model Implementation

3.1. Data

Our data, downloaded from Bloomberg, consist of the Sonia rate, as well as several OIS and interbank term rates co-observed in the Sterling market, over the five-year period from January 2016 to December 2020.[34] We work at a weekly frequency, with five business days separating each successive cross section.

Our OIS rates are collated by Bloomberg, based on quotes from multiple dealers. They correspond to single-period contracts (as considered in (10)), linked to Sonia, with terms of one, two, three, six and twelve months. Our interbank rates are the well-known, simply compounded averages (as considered in (9)) administered by the Intercontinental Exchange, known as ICE-Libor, pertaining to unsecured loans in Pound-Sterling. We again consider terms of one, two, three, six and twelve months.[35]

Key time-series are plotted in Fig. 1 above; the full dataset, along with model-fitted counterparts, are plotted in Figs. 3, 4 and C.1 below. Summary statistics of the data are given in Appendix C. We obtained the MPC meeting dates shown in these plots from the website of the Bank of England; this allows us to specify suitable quarterly jump times relative to the data time series.

We use these data over the period 2016-2019 for the estimation procedure described below, and use 2020 as an out-sample, so that the market turbulence caused by the COVID-19 pandemic does not sway our estimates. We also exclude the two- and twelve-month rates, both interbank and OIS, from the estimation; these are used as an out-of-sample interpolation and extrapolation, respectively, of the in-sample (one-, two- and six-month) term rates.

3.2. Econometric method

Our primary focus is an implementation of the model described in Section 2.3. We also consider, as comparison points, two simplified model versions: one with expected jumps only, and one only with unexpected jumps.[36]

Approximating overnight compounding with a continuous abstraction, we identify the unsecured overnight rate r_t^*, in (3), with Sonia. The modelled OIS rates (given by (11) and (12)) and inter-

[34] Sonia has undergone reform in recent history which has affected the presence of spikes in the time series. The Bank of England (BoE) took responsibility for Sonia in April 2016 but the Wholesale Market Brokers Association (WMBA) continued to calculate and publish the rate (using their previous methodology) on behalf of the BoE. The BoE then went through several rounds of consultation before implementing a methodology reform of Sonia in April 2018 and taking over all administrative duties from the WMBA. Post reform, the magnitude and frequency of spikes decreased significantly; post 2016, they are virtually absent. See Klingler and Syrstad (2021, §3).

[35] ICE also calculates overnight and weekly interbank rates. The overnight Sterling rate is extremely similar to Sonia.

[36] In these alternative models, the auxiliary state process x_t is smaller, lacking either x_t^u or x_t^e. When implementing these models, the expected- or unexpected-jump component of short-rate variation is removed from the calculation of the measurement equation in Section 3.3.

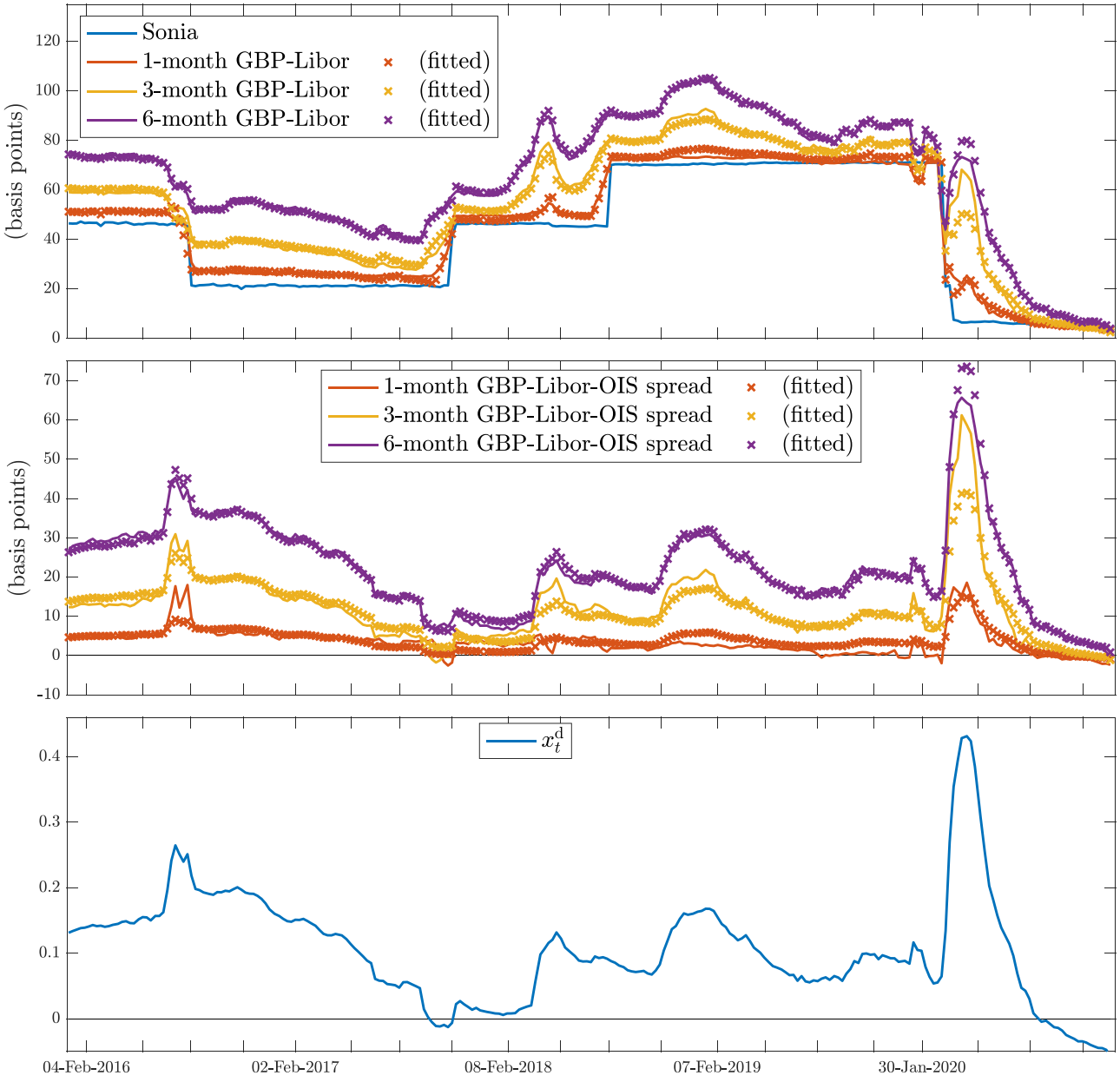

Fig. 4. A comparison of market and model-fitted interbank rates in the upper panel; a comparison of market and model-fitted Libor-OIS spreads in the middle panel; filtered state variable paths in the lower panel.

bank term rates (given by (7) and (9)) are naturally identified with the term rates described in Section 3.1.

We apply quasi maximum likelihood estimation (QMLE) in conjunction with a Kalman filter. This type of approach is widely used in the interest-rate-modelling literature, so we omit the well-known expressions detailing the filtering phases, and give only a qualitative description of the construction of the likelihood function.[37] The physical-measure dynamics of our auxiliary state processes (in (20), (21) and (22)) are discretised, giving the *transition equation*. A *measurement equation* specifies that the observed OIS and interbank rates are given by their model-implied counterparts, with the allowance for additive, zero-mean Gaussian errors, which are assumed to be independent, with standard deviation σ_{error}. The standard Kalman filter requires a linear measurement equation; ours is approximately linear (see Appendix B.1), but we use the so-called unscented Kalman filter to handle a general interest-rate pricing function.[38]

The Kalman filter provides mean-variance-optimal estimates of the state variable paths across the time series of our dataset. This separates the effects of expected and unexpected jumps on the term structure. This separation is optimal, based on how x_t^{e} and

[37] See Christoffersen et al. (2014) for a detailed treatment of the unscented Kalman filter and quasi-maximum likelihood approach in the context of term-structure modelling. See Filipović et al. (2017), Filipović and Trolle (2013) or Trolle and Schwartz (2009) for example applications.

[38] This involves discretising the conditional distribution of state variables, and transforming this distribution with the pricing function, after which one can compute the variances and covariances needed to update the state estimates based on the rates observed at that cross section. The following details would allow for an identical independent implementation of our algorithm: using the notation of Christoffersen et al. (2014), we set $\rho = 1$, $\gamma = 2$ and $\xi = \rho^2 - N$, where $N = 3$, in our parameterisation of the unscented transform, while we initialise the filtered auxiliary state variables at zero, with an initial variance of 1%.

x_t^{u} each affect the model-implied rates that feed into the measurement equation. We explain how we compute the measurement equation in Section 3.3 below, but we note here that the time inhomogeneity of the expected jumps is the conceptual key to this separation; the time until the next expected jump time is the primary determinant of whether and how x_t^{e} affects a particular term rate.

We assume that Sonia gives a direct observation of the unsecured short rate r_t^* (i.e., without measurement error), which means that the estimation of the physical-measure jump distributions is fully separable from the filtering-based likelihood. With so few Sonia jumps realised (three during 2016-2019), we do not attempt to formally estimate the physical jump distribution (in other words, we do not estimate the market price of short-rate-jump risk); see Appendix A.2 further discussion. For given parameters, the realised measurement errors imply a likelihood value based on the Gaussian density. In addition to a numerical maximum, we obtain asymptotic standard errors from the Fisher information.

The use of a Gaussian likelihood is an approximation, giving the procedure "quasi" status, because of the non-linear measurement function (and also the discretisation of the volatility dynamics in (17)). The likelihood function is robust to these approximations because it straightforwardly favours parameter sets that result in small errors, clustered around zero with a small standard deviation. To verify that our QMLE algorithm is effective and robust, we run a mock implementation on data simulated from our model. We show in Appendix B.2 that we are able to recover the parameters to an accuracy more than sufficient for practical purposes.

In terms of parameter identification, we fix the risk-adjusted intensity of unexpected jumps N_t^{u}, because this becomes entangled with the state value x_t^{u} (a lower intensity results in a proportionally higher value for x_t^{u}, in a way that cannot be separately resolved with term rate information). In particular, we set $\nu^{\mathrm{u}} = 4$, so that four unexpected jumps are experienced each year in risk-adjusted expectation, equal to the number of expected jumps; this makes the expected- and unexpected-jump variables x_t^{e} and x_t^{u} easily comparable. We set $\nu^{\mathrm{d}} = 12$, so that one credit jump is experienced per month, in risk-adjusted expectation.[39]

Recall from Section 2.3 that p_*^i controls jump variance. Jump variance is not identifiable from the term rates in our data, which depend strongly on jump mean but not on variance. Therefore, based on an informal reading of the Sonia data, we fix $p_*^i = \frac{13}{16}$, for each i. For the expected jumps, $i = \mathrm{e}$, this reflects the three non-zero Sonia jumps, and thirteen zero jumps, experienced over the sixteen MPC meetings that took place in the in-sample period 2016-2019. The unexpected jumps, corresponding to $i = \mathrm{u}$ and $i = \mathrm{d}$ remain comparable to expected jumps (and the state variables x_t^{u} and x_t^{d} comparable to x_t^{e}). Although informal, this should imbue the model with a reasonable and realistic degree of volatility; an assessment of the degree of volatility that is ultimately exhibited by the model, given in Section 3.5, is an important model validation step.[40]

3.3. Numerical pricing

We compute model-implied term rates with finite-difference methods. We detail our algorithm in Appendix B.1 (and demonstrate its agreement with a high-sample Monte-Carlo benchmark), and give a qualitative summary here. Starting with the straightforward terminal conditions $P_{TT}^L = P_{TT}^* = 1$, (7) and (12) are computed by discretising their associated Feynman-Kac partial integro-differential equations (PIDEs). Once the range of the state variables is truncated and conditions along the boundaries are specified, an iterative backwards recursion follows from the discretised PIDEs (which reflect the differing discount rates appearing in (12) and (7)). Similar to Andersen and Bang (2020), we exploit the independence between various aspects of our model by reducing one high-dimensional scheme into three two-dimensional component schemes.

In most respects, this kind of method is standard and well known; we are not aware, however, of a finite-difference implementation of expected jumps in the term-structure modelling literature. When a known jump time $s \in \mathcal{T}$ is encountered in the backwards recursion, pre-jump values are given by an expectation over the post-jump possibilities:

$$P_{s^- T}^i = \mathbb{E}_{s^-}\left[P_{s^+ T}^i\right]$$

for $i = *$ and L, which is well approximated over the discretised range of $r_{s^+}^*$ values. This component becomes time inhomogeneous, as the relationship between the loan maturities and the grid of expected jump times changes from week to week.[41]

We therefore implement the scheme ten separate times, corresponding to ten time gaps between loan maturity and the first expected jump encountered when iterating backwards in time.[42] The gap in any particular instance is between zero and one quarter (with the expected jumps occurring quarterly), so ten sample points over this range allows us to interpolate any particular value without significant error.[43]

3.4. Fitted model

The parameter values we obtain from QMLE are shown in Table 3. Consider first the expected-jump parameters, which feed into x_t^{e} (which in turn feed into the distribution of expected short-rate jumps J_t^{e}). The parameter β^{e}, which gives x_t^{e} a level-dependent volatility, is positive and significant relative to its standard error. It is also significant in the sense of providing, on average, approximately one third of the total volatility of x_t^{e} (with the constant, non-state-dependent term σ^{e} giving the other two thirds). The negative market-price-of-risk parameter μ^{e} reflects the fact that our filtered path for x_t^{e} is more positive than negative (during the in-sample period, which excludes 2020).

The unexpected-jump process x_t^{u} is estimated to be less volatile than x_t^{e}, but we shall see that it plays an important contribution in the model fit. Mild mean reversion, to a significant positive mean, is exhibited by x_t^{u}. The positive market-price-of-risk parameter reflects that this reversion does not occur in the time series, i.e., OIS rates are set as if x_t^{u} is going to revert up to the positive θ^{u} value, but under the physical-measure the mean is in fact slightly negative.

Before considering the downgrade risk parameters associated with x_t^{d}, see Fig. 3: in the lower panel, we show the estimated

[39] A value of $\nu^{\mathrm{d}} = 4$ proved inadequate for matching market Libor-OIS spreads. Our jump means are bounded, as per (16), so the jump intensity must be large enough to prevent this bounding from being restrictive.

[40] Volatility in our model comes from the jump distribution (15) and also variation of the state variables via (17), (18) and (19). The former is specified informally via p_*^i and then validated; the latter is directly informed in the estimation.

[41] We note that this type of time inhomogeneity (namely, changing position relative to jump times) is quite different from time-inhomogeneous models that are designed to fit a given term structure. One could apply the latter idea here, as per Brigo and Mercurio (2001), by re-writing (3) as $dr_t^* = J_t^{\mathrm{e}}\, dN_t^{\mathrm{e}} + J_t^{\mathrm{u}}\, dN_t^{\mathrm{u}} + df(t)$, where $f(\cdot)$ is a deterministic function used to fit the term structure. Because our model is level-independent, $f(\cdot)$ is easily obtained from $P_{tT}^{\mathrm{M}} = P_{tT}^* e^{-\int_t^T f(u)\, du}$, where P_{tT}^{M} is a given market bond price and P_{tT}^* is the pre-adjusted model bond price.

[42] On each of these implementations, we iterate backwards until all terms under consideration, with twelve months being the largest, are covered.

[43] When a jump is very near (within one tenth of one quarter), the one- or two-month rate must in fact be extrapolated from the two sample points with the lowest time-until-jump; in other words, one must take care to avoid interpolating over the discontinuous jump time.

Table 3
Quasi-maximum likelihood parameter estimates, including asymptotic standard errors in parentheses.

Model aspect		Expected Jumps	Unexpected Jumps	Downgrade
State variables		x_t^{e}	x_t^{u}	x_t^{d}
Superscript		e	u	d
Model parameters	κ	-	0.2731	2.3075
			(0.0462)	(0.1376)
	θ	-	0.4254	0.0832
			(0.0734)	(0.0048)
	σ	0.1305	0.0731	0.0793
		(0.0044)	(0.0075)	(0.0023)
	β	1.8940	-	-
		(0.2905)		
	μ	-0.5292	1.6599	-0.4922
		(0.2718)	(0.3070)	(0.4492)
$\sigma_{\text{error}} \times 10^4$		1.5552		
Log-likelihood $\times 10^{-3}$		10.0705		

paths for x_t^{e} and x_t^{u}, whereas in the upper panel, we plot the fitted OIS rates corresponding to these paths, overlaid on the market OIS rates. One can see how x_t^{e} took significant departures from its reset value of zero on five occasions: before the three non-zero expected jumps in Sonia (reflecting market views about the upcoming jump, as priced into OIS rates), before an expected jump date (i.e., MPC meeting) in May 2018, and around the unexpected, pandemic-related Sonia jump in early 2020. This occasional sudden growth of x_t^{e} accords well with its volatility dynamics in (17). The filtered path for x_t^{u}, on the other hand, appears time homogeneous, in accordance with (18). Recall that the filter, described in Section 3.2, identifies optimal values for x_t^{e} and x_t^{u} (i.e., separating the effects of expected and unexpected jumps on the term structure), based on their differing (and in one case time-inhomogeneous) effects on the OIS term structure. Recall also that the intensity of unexpected jumps is set to four, so that x_t^{e} and x_t^{u} are easily comparable in their effect on the OIS term structure; x_t^{u} can be seen to be responsible for a significant minority of the variation of OIS-Sonia spreads.

One can see that a close fit to the OIS data is attained, including in the 2020 out-sample period, with the mean absolute fitting error being under 0.7bps. We particularly wish to highlight that the fit is close in the run-up to expected jump times, when, occasionally, OIS rates take sudden departures from Sonia. These departures can be highly dependent on term; our model captures this accurately. In March and April 2018, for example, the time inhomogeneity of the model (informed by the clearly time-inhomogeneous market perception of Sonia variation) is evident, with one-month rates initially unaffected by the approaching potential jump, while the three- and six-month rates rose rapidly.

Fig. 3 further highlights the state variable level $|x_t^i| = \frac{1}{3}$, which corresponds to a risk-adjusted jump mean of twenty-five bps, via (16). While the three 25bps expected jumps were clearly anticipated in OIS rates, their ex-ante expected size was never exactly 25bps. For example, just a few days before the August-2018 jump, the one-month OIS-Sonia spread was 20bps; on the other hand, if the upcoming jump was known to be 25bps (exactly or in risk-adjusted expectation), this spread would have to exceed 22bps (because more than 90% of the one-month term falls after the jump time).

Fig. 4 shows our fit to Libor; the upper panel compares market and model-fitted interbank rates. The fit is close, with the mean absolute fitting error slightly exceeding one basis point. The middle panel shows the term structure of Libor-OIS spreads, while the bottom panels shows the filtered path for the downgrade auxiliary variable x_t^{d}, which models spread variation. A crucial aspect of the market spreads is their largely time-homogeneous behaviour. Although some time inhomogeneity is arguably evident around the first two realised jumps, in August 2016 and November 2017, and perhaps once again in 2018, this appears to be a relatively minor feature, in accordance with our time-homogeneous specification (14) and (22) (although it would be straightforward to add an expected jump component to (14)). The volatility of x_t^{d}, shown in Table 3, is relatively small, and would increase significantly if 2020 were included in the in-sample period.

Appendix C (see Fig. C.1) shows that the model also implies a close fit to the out-of-sample two- and twelve-month OIS rates. The twelve-month interbank rate, in particular, is well matched, considering that there is a significant extrapolation from the six-month term rate (included in the estimation) to the twelve-month term rate (excluded). In contrast, this out-of-sample fit is not obtained when the model is specified without unexpected jumps. Appendix C (see Fig. C.2) shows this alternative implementation, which lacks the state variable x_t^{u}. The cross-sectional, in-sample OIS fit worsens from an average root-mean-square error of 0.7bps to 0.88bps; this leads us to formally reject the nested, expected-jumps-only model, with a highly significant Newey and West (1987) t-statistic of -4.316.[44] The out-of-sample fit, especially to the twelve-month OIS rate, is significantly worse. Appendix C (see Fig. C.3) also shows an implementation of our model with only unexpected jumps, i.e., of the Babbs and Webber (1994) framework (see Section 2.3); the fit to market rates is poor, especially in the run-up to MPC meeting dates.

3.5. Interest-rate volatility and options

The option-pricing properties of our model should be of interest for several reasons: i) as discussed in Section 1, our model is well suited to capturing a realistic term structure of volatility; ii) the time-inhomogeneous effect of expected jumps on interest-rate options has not been studied; and iii) our model is able to engage with issues relating to benchmark reform, particularly reference rates being given as a function of overnight rates.

The first point is demonstrated in Table 4, where realised volatility term structures are shown. In particular, the table gives the standard deviation of weekly changes in term premium; i.e.,

$$\operatorname{std}[\Delta(R_{t,t+\tau} - r_t^*)] = \operatorname{std}\Big[(R_{t,t+\tau} - r_t^*) - (R_{t-\delta,t-\delta+\tau} - r_{t-\delta}^*)\Big], \quad (23)$$

where τ is the term in question, the first-difference operator $\Delta(\cdot)$ takes a weekly difference (so that $\delta \approx \frac{1}{50}$), and where $R_{t,t+\tau}$ is

[44] This is based on a paired t-test comparing the two models' root-mean-square pricing errors at each cross section. The scaling term is adjusted for heteroscedasticity and six-months of autocorrelation in the error series, as per Newey and West (1987)). This is a standard method for assessing cross-sectional performance of nested models; see, e.g., Filipović and Trolle (2013) and Filipović et al. (2017).

Table 4
The term structure of term premium volatility as quantified in (23), expressed in basis points. Terms range from one month (1m) to twelve months (12m).

		Term premium volatility				
		1m	2m	3m	6m	12m
OIS	Model	1.85	2.06	2.18	2.41	2.72
	Market (2016-19)	2.70	2.90	3.04	3.45	4.29
	Market (2016-20)	3.08	3.58	3.81	4.32	5.00
Libor	Model	1.90	2.21	2.45	3.01	3.77
	Market (2016-19)	2.03	2.25	2.69	3.00	3.35
	Market (2016-20)	2.96	3.60	4.33	4.75	5.03

given by either the OIS rate $\text{OIS}_{t,t+\tau}$ or the interbank rate $L_{t,t+\tau}$. The operator std[·] takes the standard deviation realised over a time series that we simulate, or over the time series constituting our data (both excluding and including 2020). The simulation method is explained in Appendix A.2; this is used to generate the time series plotted in the bottom panel of Fig. 1, which implies the model-based volatilities in Table 4 (sampling error is minor, i.e., we find only slight variation in realised volatility from one five-year simulation to another).

The primary feature of Table 4 is the increase of volatility with term. As explained in Section 1, models with a mean-reverting short rate tend to exhibit decreasing volatility term structures, whereas our model is well suited to matching this aspect of the data. Our auxiliary state process x_t causes term rates to vary, while the short end of the term structure remains unchanged. Variation is more pronounced at longer terms, as these rates are more sensitive to potential jumps.[45] In Appendix E, we show that the term structure of *implied* volatilities exhibits a similar increase.

Along with matching this pattern qualitatively, we fit the specific market volatilities reasonably well, with standard deviation values increasing from around three bps to just over four bps. Unsurprisingly, the inclusion of the 2020 pandemic-affected year (excluded from our estimation) increases volatility estimates beyond this. One interesting feature of the market data is that OIS rates are more volatile than interbank equivalents. This suggests a negative correlation between OIS rates and the Libor-OIS spread (with the addition of the spread detracting from total variation). Our model instance is unable to match this particular feature, but is certainly amenable to extension in this regard.

With volatility term structure discussed, we now consider the different rate types that could serve as underlying references and market benchmarks. To make matters concrete, consider a caplet associated with a future accrual period $[T, S]$. A traditional version of such a caplet has a time-t price proportional to[46]

$$\mathbb{E}_t\left[e^{-\int_t^S r_u^* du}(L_{TS}-K)^+\right] = \mathbb{E}_t\left[e^{-\int_t^S r_u^* du}\left(\frac{1/P_{TS}^L - 1}{S-T} - K\right)^+\right] \quad (24)$$

for $t \le S$, with the caplet referring to the interbank rate (9). If the caplet refers to the backward-looking rate (13), the time-t price is

$$\mathbb{E}_t\left[e^{-\int_t^S r_u^* du}(B_{TS}-K)^+\right] = \mathbb{E}_t\left[e^{-\int_t^S r_u^* du}\left(\frac{e^{\int_T^S r_u^* du} - 1}{S-T} - K\right)^+\right]. \quad (25)$$

[45] For expected jumps, this is because longer terms cover more expected jump times and have a longer period that the jumps could affect. Unexpected jumps are similar, as a longer term gives more opportunity for jumps to occur in a relevant time frame.

[46] Caplets are scaled according to some nominal value, while also being scaled by the length of the accrual period, here $S-T$. Note also that we have assumed the caplet to be collateralised, as we have discounted it with the unsecured rate which often serves as the collateral rate, without recognising the possibility of counterparty default.

The comparison between these two caplet types is not trivial. The backward-looking caplet benefits from the additional variation that accumulates during the accrual period; see Lyashenko and Mercurio (2019, §6.3). This can be seen as a Jensen gap between the backward-looking caplet price and the price of a forward-looking caplet linked to OIS:

$$\begin{aligned}
&\mathbb{E}_t\left[e^{-\int_t^S r_u^* du}(B_{TS}-K)^+\right] \\
&= \mathbb{E}_t\left[e^{-\int_t^T r_u^* du}\mathbb{E}_T\left[e^{-\int_T^S r_u^* du}\left(\frac{e^{\int_T^S r_u^* du}-1}{S-T} - K\right)^+\right]\right] \\
&= \frac{1}{S-T}\mathbb{E}_t\left[e^{-\int_t^T r_u^* du}\mathbb{E}_T\left[\left(1-(1+K(S-T))e^{-\int_T^S r_u^* du}\right)^+\right]\right] \\
&\ge \frac{1}{S-T}\mathbb{E}_t\left[e^{-\int_t^T r_u^* du}\left(1-(1+K(S-T))\mathbb{E}_T\left[e^{-\int_T^S r_u^* du}\right]\right)^+\right] \\
&= \frac{1}{S-T}\mathbb{E}_t\left[e^{-\int_t^T r_u^* du}P_{TS}^*(1/P_{TS}^* - 1 - K(S-T))^+\right] \\
&= \mathbb{E}_t\left[e^{-\int_t^T r_u^* du}P_{TS}^*(\text{OIS}_{TS}-K)^+\right] \\
&= \mathbb{E}_t\left[e^{-\int_t^S r_u^* du}(\text{OIS}_{TS}-K)^+\right], \qquad (26)
\end{aligned}$$

where the first and final lines are justified by simple iterated-conditioning and measurability manipulations, and where Jensen's inequality is applied to the convex payoff function.

Forward-looking caplets, on the other hand, are written on interbank rates, which are well known to exhibit spreads above OIS rates (in our model, the downgrade process appearing in (7) is responsible for modelling this spread, i.e., for ensuring that $L_{TS} > \text{OIS}_{TS}$). Even though the forward-looking caplet does not benefit from the Jensen gap, it does benefit from the Libor-OIS spread. Often, this would be accounted for with an upward-adjusted strike rate; we explain the setting of at-the-money strikes in the backward- versus forward-looking cases in Appendix E.

These effects are illustrated in Fig. 5, the upper panel of which plots caplet prices implied by our model over the sample period (i.e., we compute (24) and (25), given the fitted model in Section 3.4).[47] We initially consider caplets written on a three-month underlying rate, with three months until the start of the underlying rate's accrual period (i.e., we set $T = t + 0.25$ and $S = t + 0.5$ in (24) and (25)). The middle panel shows Bachelier implied volatilities rather than raw premia; the lower panel of the figure shows at-the-money strikes for each type of caplet.[48]

We have several comments. First, notice the (relatively minor) fluctuations in at-the-money forward-looking, Libor-linked caplet. These correspond to the fluctuations in the expected-jump state variable x_t^e in Fig. 3. When large in absolute value, its volatility increases, via the self-exciting volatility dynamics (17).[49] Option pre-

[47] We do this with 100000-sample Monte Carlo simulations, which produce short-step paths for our state variables based on their Euler-discretised dynamics. We use a step size of $\delta = \frac{1}{200}$, and trapezoidal integration. The Monte-Carlo standard error is well under 1% of the estimates themselves, and we use cross-sectionally common random numbers to ensure the Monte-Carlo error does not interfere with any comparison.

[48] We use the formulation of Lyashenko and Mercurio (2019, §6.3), where the time until expiry parameter is set as $T - t + (S-T)/3$. We do not, however, use Black implied volatilities, as these are too dependent on rate levels; the Bachelier, or Gaussian, version of the forward-Libor market model have rate-independent volatilities. At-the-money caplets have a remarkably simple premium-to-volatility relationship in the Bachelier model: for (24) and (25), $P_{t,t+S}^* \sigma_{\text{IV}} \sqrt{T^*/(2\pi)}$, with $T^* = T - t$ and $T^* = T - t + (S-T)/3$ respectively.

[49] This is the only aspect of the model with a state-dependent volatility. If removed (i.e., if $\beta^e = 0$), the forward-looking caplet becomes almost constant; minor decreases are seen when x_t^i takes a significantly non-zero value, causing a decrease to jump variance, as one side of the distribution (15) shrinks towards zero.

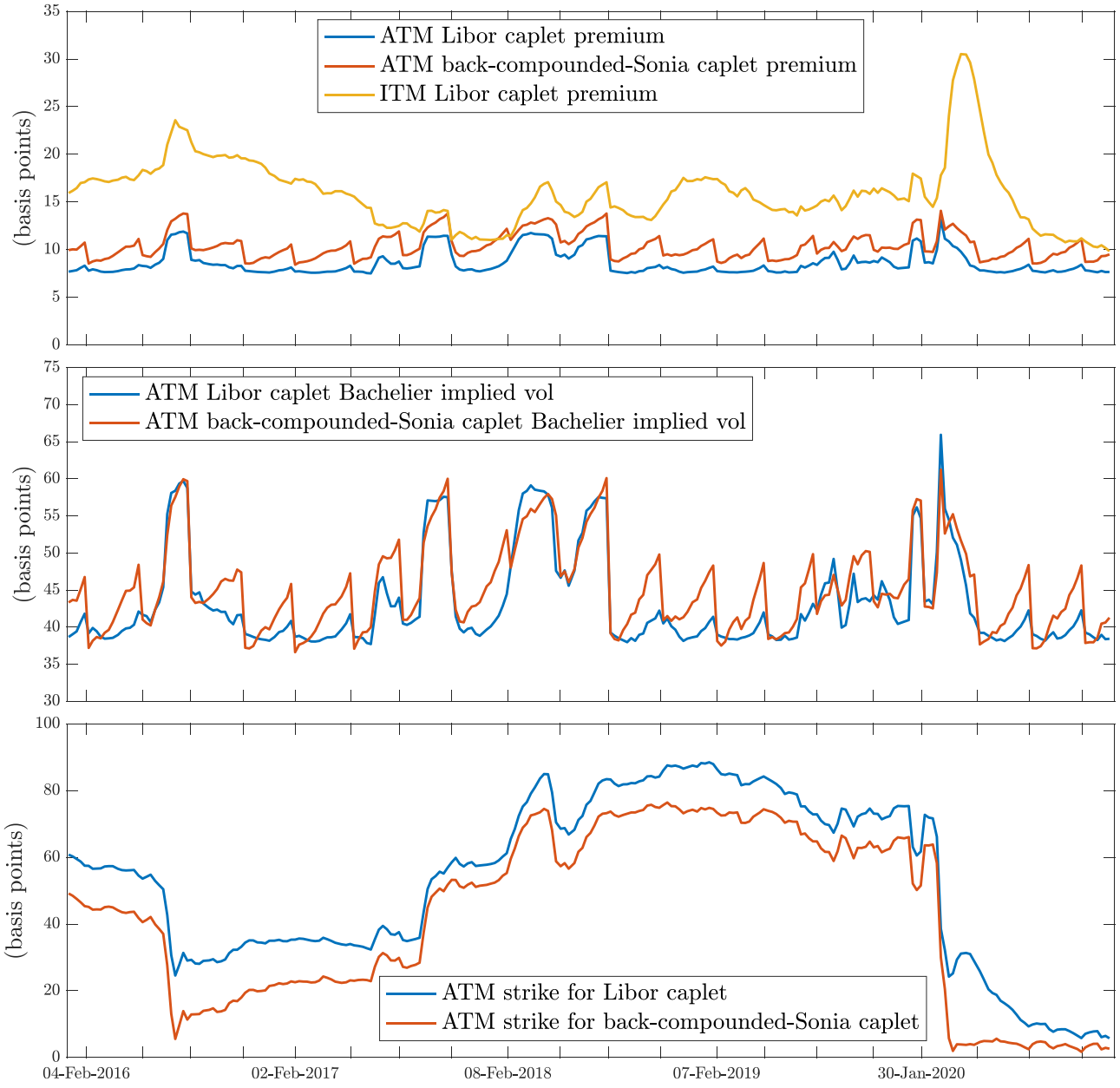

Fig. 5. A comparison of caplet premia in the upper panel; a comparison of caplet-implied volatilities in the middle panel; a comparison of at-the-money strikes rates for different caplets in the lower panel. The caplets are either at-the-money (ATM) or struck at the lower at-the-money rate of the back-compounded caplet (ITM).

mia increase as a result. There are minor fluctuations around expected jump times, just visible in the upper panel, where about 5% of option value is lost at each jump time; this is a result of the resetting of x_t^e.[50]

Second, consider the difference between the forward- and backward-looking caplets when each at-the-money (labelled ATM in Fig. 5; we address the ITM case last). The difference between the two premiums is almost all due to the Jensen gap described above.[51] The effect is significant in magnitude, but also, bringing up our third point, clearly time inhomogeneous. The backward-looking caplet premium is greatest immediately before an expected jump; this maximises potential variation of the Sonia rates that feed into the compounding formula (13), in this case allowing for two expected jumps to occur before the accrual period. Immediately after an expected jump time, only one expected jump remains relevant, in the sense of injecting variance into Sonia in a way that affects this particular (three-month backward-looking) caplet. Option values tend to drop by about 20% upon an MPC meeting date, sometimes as much as 30%, in the case of this '3x6' caplet.

The traditional, forward-looking caplets, on the other hand, are close to time homogeneous; at all times, there is one quarterly jump between the option start and when reference Libor is realised (minor variations are caused by the details of our specifica-

[50] Immediately after a jump, the reset has just occurred, and will occur again in three months before the reference Libor is realised; before a jump, the reset will shortly occur but then x_t^e is free to vary until T, which contributed to the variation of the single jump.

[51] We could give the OIS caplet in (26) to illustrate the Jensen gap directly, but this price is extremely similar to (24) (when both at-the-money). The appearance of downgrade risk in the interbank reference rate of (24) makes it slightly more variable and thus valuable, but for three-month caplets this effect is extremely minor.

tion of x_t^e as discussed above). Indeed, more generally, standardised option maturities can disguise the time-inhomogeneous effects of expected jumps. Just as these three-month caplets are effectively time homogeneous, with the particular timing of the jump in the three-month option period not being relevant, a one- or two-year forward-looking cap is not affected by a regular schedule of year times (provided the jump frequency evenly divides a year). Backward-looking caps cannot be time homogeneous though, because the timing of jumps during the accrual period is relevant (with an earlier jump resulting in more effective variation and a greater premium).

Fourthly, one can see the significance of this effect in terms of implied volatilities, as in the middle panel of Fig. 5. Bachelier implied-volatilities of the backward-looking caplet consistently drop by more than ten bps, and sometimes as much as twenty bps. Critically, one should be wary of a naive 'conversion' of one type of caplet premia to another, in terms of implied volatilities. This could be a tempting approximation for, e.g., a market maker looking to publish quotes for a new cap linked to back-compounded Sonia, based on their Libor-cap trading history. On the other hand, it would absolutely be possible to create an implied volatility transformation (other than Bachelier, such as one based on this model, or a more stylised market-style model) that adjusts for the timing of the expected jumps.

Fifth, we note that the model-implied caplet premia and their implied volatilities are in line with the premia and volatilities observed in the Sterling market. One-year cap Bachelier-implied volatilities range from twenty to forty five basis points during 2016-2020, with an average of thirty five.[52] Our obtained implied volatilities are slightly higher on average, but significantly overlapping, leading us to conclude that the degree of volatility injected by the jumps is not excessive. We therefore conclude that the swings in implied volatilities discussed in our third and fourth points above are not overstated, and that, at least around certain expected jump times, major swings in caplet premia (not only caused by realised rate jumps, but merely by the passing of time relative to the schedule of jump times) could very well prevail in a world with backward-looking benchmarks.

We acknowledge that the '3x6' caplet under consideration emphasises these time-inhomogeneous effects. In a longer term caplet, passing a jump time means losing one of many jumps, not one of two, and the premium drop is less pronounced. We show two different situations in Appendix E. On the other hand, in a market with less frequent expected jumps, or with occasional expected jumps with significantly more variance, time inhomogeneity could plausibly be much greater than shown here.

Finally, in addition to the two at-the-money cases, we consider a forward-looking caplet struck at the lower backward-looking at-the-money rate (labelled ITM in the upper panel of Fig. 5). The resultant premia are higher than at-the-money backward-looking caplet premia for virtually all of the sample, showing that the incorporation of the Libor-OIS spread is more significant than the Jensen-gap effect (other things, including strike, being equal), but there is significant variation. This variation correlates directly with the variation in the spread between the two strike prices, shown the in bottom panel of the figure (e.g., in November 2017, the Libor-OIS spread is very small, and one can see that the slightly-in-the-money Libor caplet is worth the same as the at-the-money Sonia caplet). The change from a forward-looking unsecured-borrowing term rate (which prices in rollover risk) to an artificial term rate (i.e., OIS or a back-compounded overnight rate) should not be taken lightly. If the strike rate is not carefully adjusted, the upper panel of Fig. 5 shows that the resultant change in value can be extremely significant.

[52] As in Section 3.1, this is based on Bloomberg composite quotes. Although the full time series of weekly quotes was not available, the majority exhibited this range and average.

4. Conclusion

We have introduced a modelling framework exhibiting expected (deterministically timed) and unpredictable jumps, in a modern, multi-curve setting based on interbank default. We have also specified a model instance, motivated by Sterling market data; these data are an excellent example of expected and unexpected jumps, both in the times series of overnight rates, Sonia, and the behaviour of term rates, GBP-Libor and OIS.

This model instance was implemented on this data, in the sense of a maximum likelihood estimation over the time series of the various rates. The model fits the changing OIS term structure closely, with both the expected- and unexpected-jump distributions playing an important role. Noteworthy is how the fit remains close in the run-up to expected jumps that were pre-empted by OIS rates; this would not be achieved if our model-based calculations of the expected-jump time inhomogeneity were incorrect, nor if the market did not price upcoming expected jumps into term rates. The model also fits the interbank term rates closely, with the vast majority of fitting errors being less than one basis point. An endogenous multi-curve structure (i.e., the term structure of interbank rates relative to OIS rates, and the multiple curves bootstrapped from swaps referencing interbank rates) emerges from the underlying variables of the model, rather than from an ad-hoc specification. While Libor is on the decline, these principles remain essential for modelling any kind of genuine term rate, in the sense of being associated with a loan to a fixed borrower with risk of default. Discussions around various types of interest rate benchmark, and their applicability to borrowers of different types, will doubtless touch on this issue, and our model gives a rigorous implementation thereof.

With the topicality of benchmark reform, the literature has recognised that, all else equal, backward-looking options exhibit more volatility and are thus more valuable than traditional forward-looking options; our model is able to rigorously account for this effect, which, with realistic degrees of expected and unexpected jumps exhibited in the short-term rate, can be of clear economic significance for short-term options. Moreover, this effect can be highly time inhomogeneous, as time evolves relative to a fixed schedule of expected jump times. At-the-money caplet premia, for short-term backward-looking contracts, can change more than 20% as an expected jump time passes. Traditional forward-looking caplets tend not to exhibit this time inhomogeneity, because standardised maturities result in a constant number of jumps during the life of the option; on the other hand, options linked to the ascendant backward-looking-style benchmark are necessarily time inhomogeneous with respect to expected jumps. Finally, our model provides an increasing term structure of interest-rate volatility, a feature that naturally emerges from the jumps driving short-rate variation, and is clearly exhibited by the market, allowing our model to handle contracts with different underlying accrual periods (e.g., caplets linked to three- versus six-month Libor) consistently.

Declaration of Competing Interest

None.

CRediT authorship contribution statement

Alex Backwell: Conceptualization, Data curation, Formal analysis, Investigation, Methodology, Project administration, Supervision, Validation, Writing – original draft, Writing – review & edit-

ing. **Joshua Hayes:** Data curation, Formal analysis, Investigation, Methodology, Project administration, Supervision, Writing – original draft, Writing – review & editing.

Appendix A. Measure-change details

A1. Measure-change theory

To formally introduce a risk-adjusted measure applicable to our basic framework in Section 2.1, define a process satisfying

$$\frac{dL_t}{L_{t^-}} = K_t^{\mathrm{e}}\, dN_t^{\mathrm{e}} + K_t^{\mathrm{u}}\, dN_t^{\mathrm{u}} - \bar{\nu}_t^{\mathrm{u}} \mathbb{E}_{t^-}^{\mathbb{P}}[K_t^{\mathrm{u}}]\, dt, \qquad L_0 = 1, \tag{A1}$$

where $\bar{\nu}_t^{\mathrm{u}}$ denotes the physical-measure time-t jump intensity of N_t^{u}, and where K_t^{e} and K_t^{u} are market-price-of-jump-risk variables, jumps themselves that are independent from the Poisson process N_t^{u}, that are specified in order to characterise $\mathbb{Q}$. We need J_t^{u} to be independent from N_t^{u} for the approach in this section to be effective, as J_t^{u} and K_t^{u} should not necessarily be independent.

They have to meet a few requirements, to ensure that L_t is a strictly positive martingale. It is required that K_t^{e} has zero physical expectation at an expected jump time (i.e., $\mathbb{E}_{t^-}^{\mathbb{P}}[K_t^{\mathrm{e}}] = 0$). To keep L_t positive, it is also required that $K_t^{\mathrm{e}} > -1$ and $K_t^{\mathrm{u}} > -1$.

One can then use the martingale L_t as a Radon-Nikodym derivative process, sometimes known as a likelihood process, that progressively characterises a measure change (see, e.g., Björk (2004, Appendix C.3)):

$$L_t = \left.\frac{d\mathbb{Q}}{d\mathbb{P}}\right|_{\mathcal{F}_t} = \mathbb{E}_t^{\mathbb{P}}\left[\frac{d\mathbb{Q}}{d\mathbb{P}}\right],$$

which allows time-t conditional expectations, and unconditional expectations of time-t measurable variables, to be converted to the risk-adjusted measure. Using the abstract Bayes' formula, for some function $f(\cdot)$

$$\begin{aligned}\mathbb{E}_{t^-}\left[f\left(J_t^i\right)\right] = \frac{\mathbb{E}_{t^-}^{\mathbb{P}}\left[L_t\, f\left(J_t^i\right)\right]}{L_{t^-}} &= \frac{\mathbb{E}_{t^-}^{\mathbb{P}}\left[(L_{t^-} + \Delta L_t)\, f\left(J_t^i\right)\right]}{L_{t^-}} \\ &= \mathbb{E}_{t^-}^{\mathbb{P}}\left[(1 + K_t^{\mathrm{e}}\, dN_t^{\mathrm{e}} + K_t^{\mathrm{u}}\, dN_t^{\mathrm{u}})\, f\left(J_t^i\right)\right],\end{aligned}$$

where $\Delta L_t = L_t - L_{t^-}$. Noting that $L_t = L_{t^-} + \Delta L_t = L_{t^-}(1 + K_t^{\mathrm{e}}\, dN_t^{\mathrm{e}} + K_t^{\mathrm{u}}\, dN_t^{\mathrm{u}})$, and assuming that the two types of jump do not coincide,[53]

$$\begin{aligned}\mathbb{E}_{t^-}\left[f\left(J_t^i\right) \mid dN_t^i = 1\right] &= \frac{\mathbb{E}_{t^-}^{\mathbb{P}}\left[L_t\, f\left(J_t^i\right) \mid dN_t^i = 1\right]}{\mathbb{E}_{t^-}^{\mathbb{P}}\left[L_t \mid dN_t^i = 1\right]} \\ &= \frac{L_{t^-}\mathbb{E}_{t^-}^{\mathbb{P}}\left[(1 + K_t^i\, dN_t^i)\, f\left(J_t^i\right) \mid dN_t^i = 1\right]}{L_{t^-}\mathbb{E}_{t^-}^{\mathbb{P}}\left[(1 + K_t^i\, dN_t^i) \mid dN_t^i = 1\right]} \\ &= \frac{\mathbb{E}_{t^-}^{\mathbb{P}}\left[(1 + K_t^i)\, f\left(J_t^i\right)\right]}{\mathbb{E}_{t^-}^{\mathbb{P}}\left[(1 + K_t^i)\right]}.\end{aligned} \tag{A2}$$

The denominator falls away with $i = \mathrm{e}$, from the requirements on K_t^{e}. On the other hand, $\mathbb{E}_{t^-}^{\mathbb{P}}[K_t^{\mathrm{u}}]$ may be non-zero; indeed, this plays the important role of allowing the physical and risk-adjusted intensities to differ as desired. In particular, as stated in Footnote 19,

$$\nu_t^{\mathrm{u}} = \bar{\nu}_t^{\mathrm{u}}\left(1 + \bar{\mathbb{E}}_{t^-}[K_t^{\mathrm{u}}]\right). \tag{A3}$$

One can refer to Piazzesi (2010, §3.5.3) or Shreve (2004, Ch.11.6.2) for a proof. However, we note an error in Piazzesi (2010, §3.5.3): the compensation term in measure change process (corresponding to (A1)) is incorrect in general, as it uses K_t^{u} rather than $\mathbb{E}_{t^-}^{\mathbb{P}}[K_t^{\mathrm{u}}]$ (leading to a non-predictable compensator).

Intuitively, the mean of K_t^{u}, if non-zero, is chosen to adjust jump intensity, while the variation of K_t^{u} and K_t^{e} around their means (particularly how this co-varies with J_t^{u} and J_t^{e}) is set to adjust the jump size distributions. In the context of the model in Section 2.3, with its discrete jump distribution, one can specify

$$K_t^{\mathrm{e}} = \begin{cases} \dfrac{\mathbb{Q}(J_t^{\mathrm{e}}, x_t) - \mathbb{P}(J_t^{\mathrm{e}}, x_t)}{\mathbb{P}(J_t^{\mathrm{e}}, x_t)} & \text{if } \mathbb{P}(J_t^{\mathrm{e}}, x_t) \neq 0; \\ 0 & \text{if } \mathbb{P}(J_t^{\mathrm{e}}, x_t) = 0, \end{cases}$$

where $\mathbb{P}(j, x) = \mathbb{P}(J_t^{\mathrm{e}} = j \mid x_{t^-} = x)$, from the initially specified conditional distribution of the jumps under $\mathbb{P}$, and where $\mathbb{Q}(\cdot,\cdot)$ is the desired risk-neutral probability mass function for J_t^{e} (which must be zero when the corresponding $\mathbb{P}$ probability is zero, to ensure that $K_t^{\mathrm{e}} > -1$). This can be verified by considering $f\left(J_t^{\mathrm{e}}\right) = \mathbb{I}(J_t^{\mathrm{e}} = j)$ in (A2), for any jump size j. The same approach can be used for unexpected jumps J_t^{u}, with an adjustment given the potential effect of the denominator in (A2).

For the model described in Section 2.3, a Brownian motion is used to drive x_t, and another compounded Poisson process $J_t^{\mathrm{d}}\, dN_t^{\mathrm{d}}$ is used to drive downgrade risk. A generalisation of (A1) is then required:

$$\begin{aligned}\frac{dL_t}{L_{t^-}} = {} & K_t^{\mathrm{e}}\, dN_t^{\mathrm{e}} + K_t^{\mathrm{u}}\, dN_t^{\mathrm{u}} - \bar{\nu}_t^{\mathrm{u}} \mathbb{E}_{t^-}^{\mathbb{P}}[K_t^{\mathrm{u}}]\, dt + K_t^{\mathrm{d}}\, dN_t^{\mathrm{d}} \\ & - \bar{\nu}_t^{\mathrm{d}} \mathbb{E}_{t^-}^{\mathbb{P}}[K_t^{\mathrm{d}}]\, dt + \mu_t\, d\bar{W}_t,\end{aligned}$$

again with $L_0 = 1$, where μ_t is the three-dimensional market-price of risk process used in (17), (18), (19). The intensity relationship (A3) applies (i.e, u can be replaced with d), as does the expectation relationship (A2) (i.e, one can set $i = \mathrm{d}$).

A2. Simulation discussion

We first clarify our treatment of the physical-measure jump distributions. Sonia is the starting point of our model; recall that we use Sonia as a direct observation of r_t^*, i.e., we assume zero measurement error. The term rates are measured with noise characterised by σ_{error}, requiring us to filter terms rate to estimate the path of x_t. This brings the physical dynamics into the filter-based likelihood value. The risk-adjusted jump distribution is also a key contributor to the likelihood, but, given the value of r_t^* at each cross section, the physical jump distribution is not.

With only a small handful of realised non-zero jumps, we have estimated the jump distribution informally (with the non-zero-jump probability $1 - p_*^{\mathrm{e}}$ informed by the tally of jumps, and the discrete jump possibilities guided by the realised jumps). We then maintain this distribution under the risk-adjusted measure (specifically the support of this distribution; the physical mean need not conform to (16), and the physical probability of a zero jump need not be p_*^{e}). It is conceivable for there to be more jump volatility under $\mathbb{Q}$ (i.e., it is conceivable that a lower p_*^{e} value could be suitable, as this is guided by a physically realised path), but we cannot ascertain this from term rates (which are virtually indifferent to volatility), and we wish to avoid overstated volatility for our Section 3.5 (which we seem to have done, given that our obtained caplet-implied volatilities are in line with the short-term cap market). We have extended this informally determined distribution to the unexpected jumps, although of course they are controlled by a separate state variable x_t^{u}.

Note that all of Section 3 is compatible with any physical jump distribution (provided it is equivalent, in the sense of agreeing on null jump realisations). In order to simulate a path of our model, however, we must fix a physical distribution. We do this for the purposes of Fig. 1, Table 4 and Appendix B.2 (which are all based on the same simulation). We let $\mathbb{P}$ and $\mathbb{Q}$ distributions coincide, with one exception: we reduce $\bar{\nu}^{\mathrm{u}}$ (the physical intensity of unexpected jumps) to one (which is mathematically consistent, via (A3)). Recall that we set ν^{u}, the $\mathbb{Q}$ intensity, to four, in order to make x_t^{e} and x_t^{u} easily comparable (with four expected jumps per

[53] More formally, $\mathbb{E}_{t^-}[\cdot \mid dN_t^i = 1]$ is $\mathbb{E}[\cdot \mid \mathcal{F}_{t^-} \vee dN_t^i = 1]$.

year). But this intensity under $\mathbb{P}$ results in far too many unexpected jumps over the time series (in particular, $(1-\frac{13}{16})\times 4\times 5\approx 4$ non-zero jumps over a five-year period, where one is realised in our sample). Note that this intensity adjustment does not bear on Table 4 or Appendix B.2 (which depend on term premium above the short rate, but not the short rate itself), but only on the look of Fig. 1.

Our simulation is based on our estimated parameters in Table 3. We use a weekly Euler discretisation of the x_t dynamics (20), (21) and (22), and standard random sampling of $\bar{W}_t$, J^{e}_t, J^{u}_t and N^{u}_t.

Appendix B. Implementation details

B1. Numerical pricing

Given some fixed $t\geq 0$, define r^{e}_s and r^{u}_s to satisfy

$$dr^{\mathrm{e}}_s = J^{\mathrm{e}}_s\, dN^{\mathrm{e}}_s \quad r^{\mathrm{e}}_t = r^*_t,$$
$$dr^{\mathrm{u}}_s = J^{\mathrm{u}}_s\, dN^{\mathrm{u}}_s, \quad r^{\mathrm{u}}_t = 0,$$

so that $r^*_s = r^{\mathrm{e}}_s + r^{\mathrm{u}}_s$ for $s\geq t$. Using the independence properties of our model, the Libor discount factor (7) can be given as[54]

$$\begin{aligned} P^L_{tT} &= \mathbb{E}_t\left[e^{-\int_t^T (r^{\mathrm{e}}_u + r^{\mathrm{u}}_u + \lambda^{(t)}_u)du}\right] \\ &= \mathbb{E}_t\left[e^{-\int_t^T r^{\mathrm{e}}_u du}\right]\mathbb{E}_t\left[e^{-\int_t^T r^{\mathrm{u}}_u du}\right]\mathbb{E}_t\left[e^{-\int_t^T \lambda^{(t)}_u du}\right] \\ &= f(t,T,r^{\mathrm{e}}_t,x^{\mathrm{e}}_t)\; g(t,T,r^{\mathrm{u}}_t,x^{\mathrm{u}}_t)\; h(t,T,\lambda^{(t)}_t,x^{\mathrm{d}}_t), \end{aligned} \tag{B1}$$

where the Markov property of each pair of variables (e.g., r^{e}_t and x^{e}_t are jointly Markov, with x^{e}_t feeding into jump driving r^{e}_t). As is well known, the functions f, g and h each solve a partial integro-differential equation (PIDE) associated with the expectations in (B1).[55] In particular, assuming $s\in(t,T)$ is not an expected jump time,

$$\partial_s f(s,T,r,x) + \frac{1}{2}\partial_{xx} f(s,T,r,x)(\sigma^{\mathrm{e}} + \beta^{\mathrm{e}}|x|)^2 = r f(s,T,r,x), \tag{B2}$$

$$\begin{aligned} &\partial_s g(s,T,r,x) + \partial_x g(s,T,r,x)\kappa^{\mathrm{u}}(\theta^{\mathrm{u}} - x) + \frac{1}{2}\partial_{xx} g(s,T,r,x)(\sigma^{\mathrm{u}})^2 \\ &\quad + \nu^{\mathrm{u}}\mathbb{E}_{s^-}[\Delta g(s,T,r^{\mathrm{u}}_{s^-} + J^{\mathrm{u}}_s, x^{\mathrm{u}}_s)] = r g(s,T,r,x), \end{aligned} \tag{B3}$$

$$\begin{aligned} &\partial_s h(s,T,r,x) + \partial_x h(s,T,r,x)\kappa^{\mathrm{d}}(\theta^{\mathrm{d}} - x) + \frac{1}{2}\partial_{xx} h(s,T,r,x)(\sigma^{\mathrm{d}})^2 \\ &\quad + \nu^{\mathrm{d}}\mathbb{E}_{s^-}\left[\Delta h(s,T,\lambda^{(t)}_{s^-} + \max(J^{\mathrm{d}}_s, -\Lambda_s), x^{\mathrm{d}}_s)\right] = r h(s,T,r,x), \end{aligned} \tag{B4}$$

given the dynamics in (3), (14), (17), (18) and (19). Note that r and x are generic placeholder variables above; r represents the 'discount rate' in each expectation in (B1).

We compute f as follows. Beginning at the known terminal condition $f(T,T,r,x)=1$, we use a discretised version of the PIDE (B2) to approximate $f(T-\delta,T,r,x)$ over a grid of values for the variables r^{e}_t and x^{e}_t, where $\delta>0$ is some small time step. In particular, we treat x^{e}_t implicitly, meaning that x-derivatives are taken at the new, back-stepped time point (whereas f itself is averaged over the time current and new time points). This leads to a set of linear equations that can be solved to give the new f values in terms of the known current ones. This process is then iterated until an expected jump time is encountered, or until the desired distance from the terminal condition (corresponding to the underlying term $T-t$). Upon an expected jump time $s\in\mathcal{T}$, the following step must be inserted into the iteration:

$$\begin{aligned} f(s^-,T,r^{\mathrm{e}}_{s^-},x^{\mathrm{e}}_{s^-}) &= \mathbb{E}_{s^-}[f(s,T,r^{\mathrm{e}}_{s^-} + J^{\mathrm{e}}_s, 0)] + \\ &= \mathbb{E}_{s^-}[f(s,T,r^{\mathrm{e}}_s, 0)], \end{aligned} \tag{B5}$$

recalling the resetting $x^{\mathrm{e}}_s = 0$ specified in (17).[56] This ensures that $\mathbb{E}_{t^-}[\Delta f(s,T,r^{\mathrm{e}}_s, x^{\mathrm{e}}_s)] = 0$, i.e., an expected jump cannot cause an instantaneous non-zero profit or loss in expectation (the definition of f in (B1) requires that instantaneous expected profits are infinitesimal, arriving at *rate* r^{e}_s). Given our discrete jump distribution, we can calculate the right-hand side of (B5) for each pre-jump pair $(r^{\mathrm{e}}_{s^-}, x^{\mathrm{e}}_{s^-})$ directly off the post-jump grid. While this is a simple application of PIDE theory, we are not aware of expected jumps being incorporated into a finite-difference method in the finance literature.

A similar process is used to compute g and h. We again treat x^{u}_t and x^{d}_t implicitly. Expected jump insertions are not needed, but post-jump averaging is needed at each step of the algorithm in order to incorporate the jump term in (B3) and (B4). In the case of g, we compute the following for each pair $(r^{\mathrm{u}}_{s^-}, x^{\mathrm{u}}_{s^-})$:

$$\begin{aligned} &\mathbb{E}_{s^-}[\Delta g(s,T,r^{\mathrm{u}}_{s^-} + J^{\mathrm{u}}_s, x^{\mathrm{u}}_s)] \\ &\quad = \mathbb{E}_{s^-}[g(s,T,r^{\mathrm{u}}_{s^-} + J^{\mathrm{u}}_s, x^{\mathrm{u}}_s)] - g(s^-,T,r^{\mathrm{u}}_{s^-}, x^{\mathrm{u}}_{s^-}). \end{aligned} \tag{B6}$$

Along with implicit finite-difference approximations for the x-derivatives (taken at $s-\delta$), one can solve the discretised version of (B3).

Both g and h are time homogeneous, i.e.,

$$g(t,T,r,x) = g(t+\tau, T+\tau, r, x),$$

for any $\tau\geq -t$, so their iteration algorithms only need to be run once per parameter set. On the other hand, f is time inhomogeneous, requiring its algorithm to be run numerous time, as described in Section 3.3. The downgrade component in (B1), h, can be excluded in order to compute the OIS discount factor (12). We note that $g(t,T,r^{\mathrm{u}}_t,x^{\mathrm{u}}_t) = g(t,T,0,x^{\mathrm{u}}_t)$ and $h(t,T,\lambda^{(t)}_t,x^{\mathrm{d}}_t) = h(t,T,0,x^{\mathrm{d}}_t)$, given the definitions of r^{u}_t and $\lambda^{(t_0)}_t$.

We truncate r^{e}_t, r^{u}_t and $\lambda^{(t)}_t$ (the first spatial variable in f, g and h) at -1% and -3%. Near these boundaries, jumps can potentially leave the truncated region, so a linear extrapolation is used to calculate (B5) and (B6). We truncate each x^i_t at -1.25 and -1.25, which is well beyond the $[-0.5, 0.5]$ range in which they affect the jump distribution (recall Table 2). Errors at the boundaries accumulate if this truncation is too narrow. At these x^i_t-boundaries, we enforce a Neumann boundary condition, namely that the slope exhibited over the final two nodes continues beyond the truncation boundaries.

We use a time-step of $\delta = \frac{1}{360}$, which divides conveniently into the monthly terms and quarterly expected jumps. For the spatial variables, we use a step size of five bps to construct the grids. To validate the effectiveness of this algorithm, we compare the results to 50000-sample Monte-Carlo computations of (B1), where the state-variable dynamics are simulated with an Euler discretisation with step size of 0.0005, using our estimated parameters in Table 3. Fig. B.1 considers varying each variable, while keeping the others at the central value in the plot ($r^*_t = 0.01$ and $x^i_t = 0$), and shows a close agreement of the two approaches. A three-month term is considered, with an expected jump in the middle of this term. Table B.1 shows the values of absolute errors from Fig. B.1. These errors are tiny, seldom above a tenth of a basis point, providing high confidence that our finite-difference bond pricer is sufficiently accurate. While Monte-Carlo simulation is effective for a

[54] Expected and unexpected jumps can be separated because their conditional distributions are independent of the short rate, and of x^{u}_t and x^{e}_t respectively. If *both* jumps depends on the short rate, or if there was expected-unexpected cross dependence, we would have to solve a three-dimensional scheme, which is significantly slower but still tractable on a typical computer.

[55] See, e.g., Crepey (2013, Ch. 3) for rigorous derivation of the PIDE form, and Crepey (2013, Ch. 8) for a detailed treatment of finite-difference methods we use to numerically solve them.

[56] This can be seen as the standard risk-neutral formula, over the instantaneous jump time: $f(s^-,T,r^{\mathrm{e}}_{s^-},x^{\mathrm{e}}_{s^-}) = \mathbb{E}_{s^-}[e^{-\int_{s^-}^{s} r^{\mathrm{e}}_u du} f(s,T,r^{\mathrm{e}}_s,x^{\mathrm{e}}_s)]$.

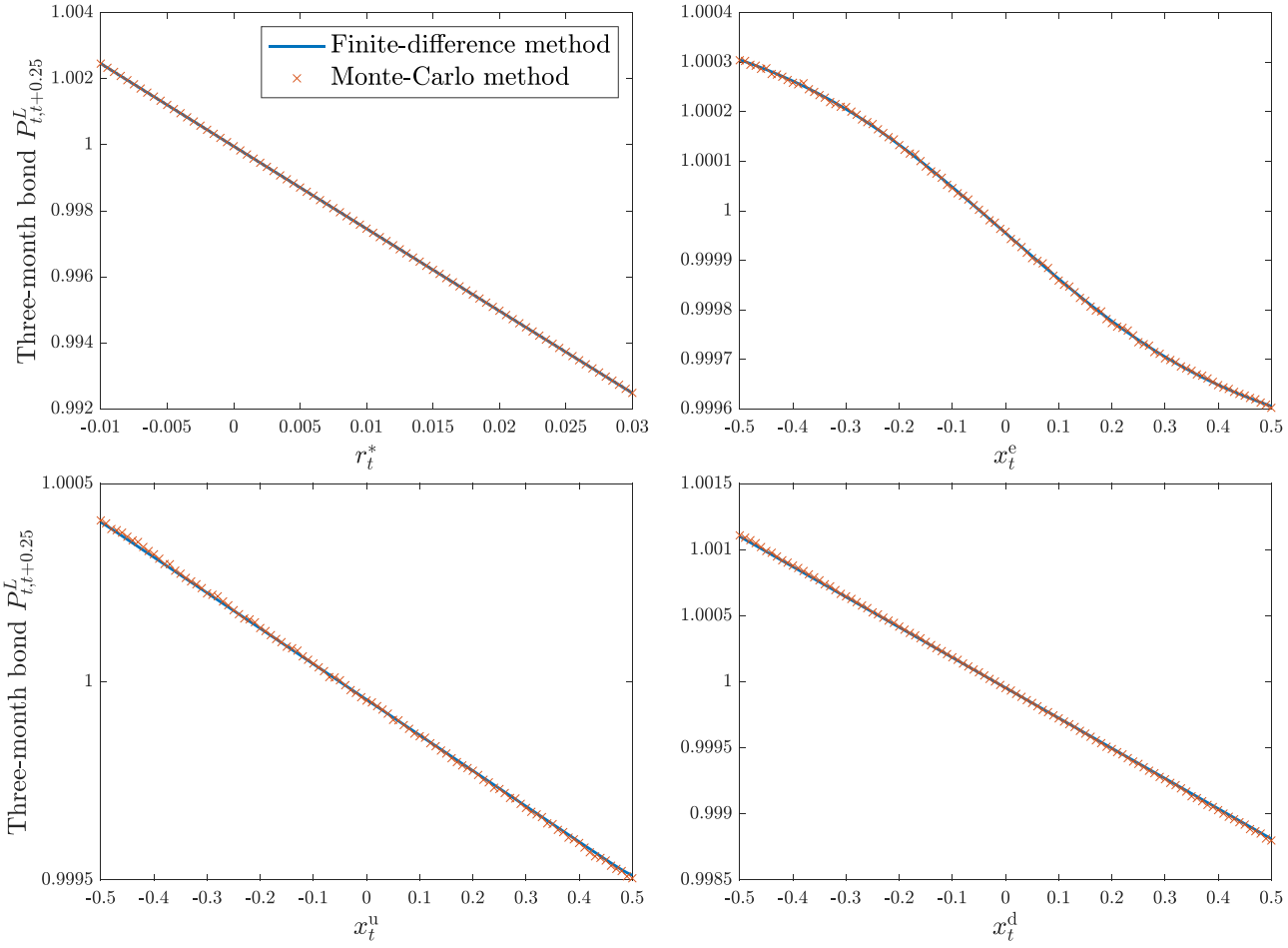

Fig. B1. A comparison of finite-difference- and Monte-Carlo-based computations of a three-month Libor discount factor.

Table B1
Pricing errors, in absolute terms (Abs.), for a three-month Libor discount factor, comparing finite-difference- and Monte-Carlo-based computations. The four state variables are each varied away from zero. The errors are expressed in basis points, relative to a discount factor approximately equal to one.

Value of r^*_t	-0.01	0	0.01	0.02	0.03
Abs. error (bps)	0.0113	0.00810	0.0181	0.0686	0.0278
Value of x^e_t	-0.5	-0.25	0	0.25	0.5
Abs. error (bps)	0.0083	0.0396	0.0239	0.0467	0.0342
Value of x^u_t	-0.5	-0.25	0	0.25	0.5
Abs. error (bps)	0.0473	0.0129	0.0244	0.0133	0.0768
Value of x^d_t	-0.5	-0.25	0	0.25	0.5
Abs. error (bps)	0.0854	0.0146	0.0231	0.0415	0.1277

Table B2
Quasi-maximum likelihood parameter estimates on data simulated by our model with the parameters from Table 3.

Model aspect		Expected Jumps	Unexpected Jumps	Downgrade
State variables		x^e_t	x^u_t	x^d_t
Superscript		e	u	d
Model parameters	κ	-	0.5753	2.2732
	θ	-	0.3507	0.0808
	σ	0.1440	0.0661	0.0935
	β	1.5767	-	-
	μ	-0.8779	3.3089	0.0904
$\sigma_{\text{error}} \times 10^4$		1.9050		

single bond price, it does not scale well for our problem, which requires many bond price computations for each parameter set. A finite-difference scheme can be run once per parameter set (as the output covers all initial states), resulting in a substantial saving in computational cost.

B2. Quasi-likelihood validation

Table B.2 shows the results of our estimation algorithm (described in Section 3.2) applied to the simulated data in Fig. 1 (as discussed in Appendix A.2) with the addition of Gaussian noise as per the estimated σ_{error}. Comparing to Table 3 (which governs the simulation), the filter-based algorithm appears to provide robust estimates, despite its "quasi"-maximum likelihood status. We note a minor identification issue with the unexpected jumps component of our model: the estimates for κ^u and θ^u in Table B.2 are slightly higher and lower, respectively, than their counterparts in Table 3. This results in a virtually identical term-rate fit; with the underlying values, x^d_t reverts a little less strongly to a slightly higher value, resulting in, crucially, very similar $\mathbb{Q}$-expectations.

Appendix C. Supplementary results

Table C.1 provides summary statistics of our market data described in Section 3.1.

Fig. C.1 shows the out-of-sample fit of the model to the two- and twelve-month term rates (for both Libor and OIS). Recall that the model takes one-, three-, and six-month term rates as inputs. One can think of the two-month rate being interpolated be-

Table C1
Summary statistics of the market data (bps), where Δ denotes a weekly first-order difference of the rate in question. Terms range from one month (1m) to twelve months (12m) for both Libor and OIS rates.

	Sonia			Libor			OIS				
	ON	1m	2m	3m	6m	12m	1m	2m	3m	6m	12m
					2016–2019						
$\mathbb{E}[r]$	47.09	50.80	54.82	59.78	71.45	89.86	47.24	47.59	47.85	48.68	51.14
$\mathbb{V}\text{ar}[r]$	20.18	18.84	18.94	20.04	18.38	15.65	20.20	20.18	20.19	20.42	21.79
$\mathbb{E}[\Delta r]$	0.12	0.10	0.10	0.10	0.06	-0.04	0.12	0.12	0.11	0.09	0.04
$\mathbb{V}\text{ar}[\Delta r]$	2.83	1.52	1.48	1.66	1.76	2.31	1.70	1.61	1.69	2.13	3.25
					2016–2020						
$\mathbb{E}[r]$	41.39	44.69	48.86	53.63	64.35	81.25	41.27	41.44	41.56	41.90	43.33
$\mathbb{V}\text{ar}[r]$	24.14	23.25	23.44	25.02	25.31	25.94	24.03	24.09	24.15	24.63	26.55
$\mathbb{E}[\Delta r]$	-0.17	-0.19	-0.21	-0.23	-0.29	-0.39	-0.17	-0.17	-0.17	-0.18	-0.22
$\mathbb{V}\text{ar}[\Delta r]$	4.14	2.57	2.81	3.00	3.02	3.38	3.04	2.91	2.92	3.07	3.69

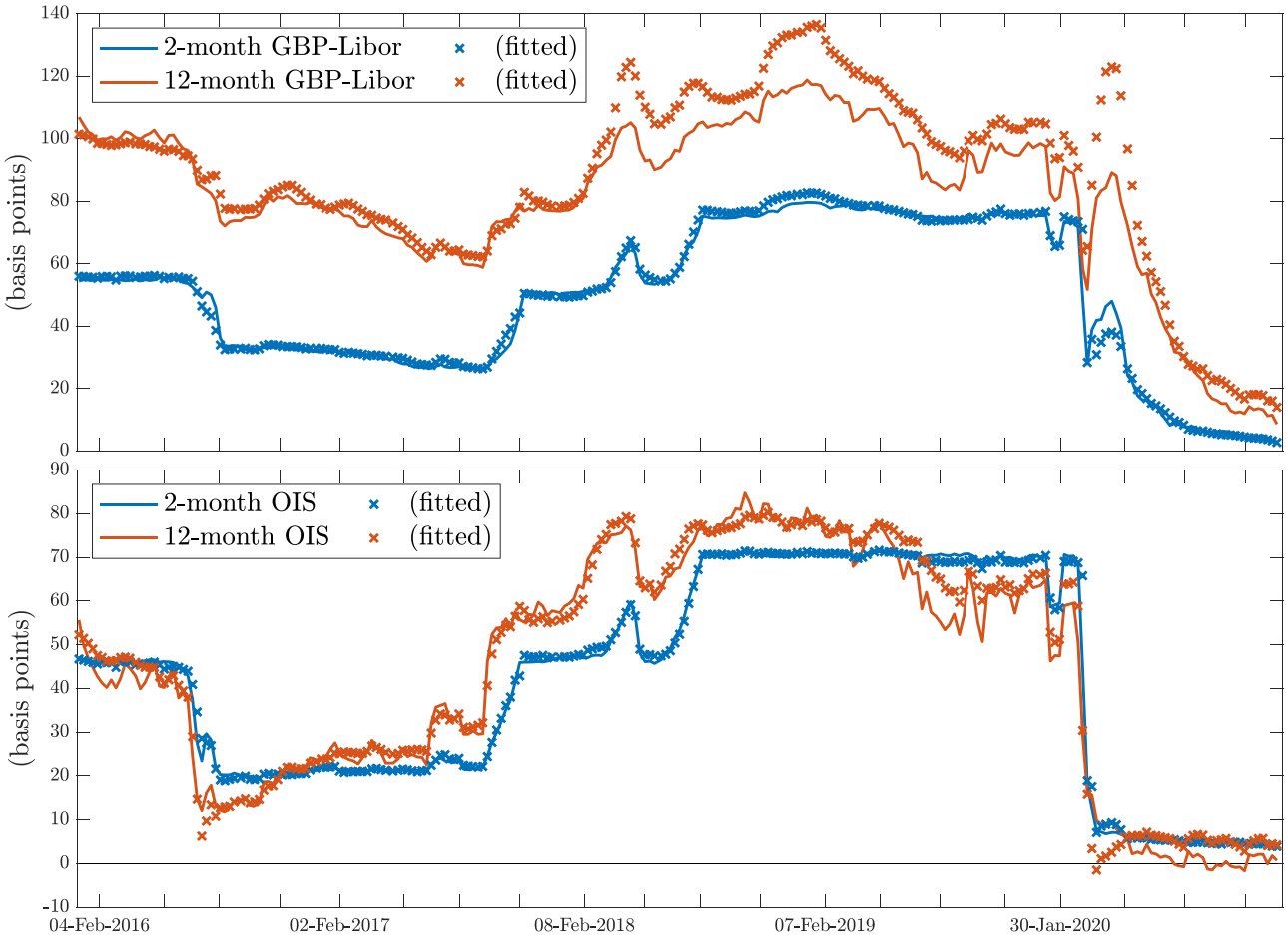

Fig. C1. A comparison of market and model-fitted interbank (OIS) rates in the upper (lower) panel. These rates were not included in the estimation of the model.

tween the data-informed points, whereas the twelve-month rate is extrapolated beyond the observed six-month term horizon. Neither rate was used for the main estimation of the parameters in Table 3.

Fig. C.2 shows the in- and out-of-sample fits to OIS rates of an alternative implementation of the model which has only an expected jumps component. This model therefore removes any influence of the state variables x_t^{u} and x_t^{d}. Looking at the twelve-month term rate in the upper panel indicates that this version of the model completely fails to provide a convincing out-of-sample fit to this rate. Table C.2 provides the QMLE estimates of the parameters corresponding to the alternative implementation of the model giving rise to Fig. C.2.

Fig. C.3 shows in- and out-of-sample fits to OIS rates of the model with unexpected jumps only, in line with the framework set out in Babbs and Webber (1994). Without the time inhomogeneity resulting from the expected jump dates, this model struggles to fit OIS rates in the run-up to expected jumps (as the model cannot match the time-inhomogeneous effect across various terms). Like the expected-jumps-only model (but unlike the full model, as in Fig. C.1), the fit to the twelve-month OIS rate is very poor. The parameters giving rise to Fig. C.3 can be found in Table C.2.

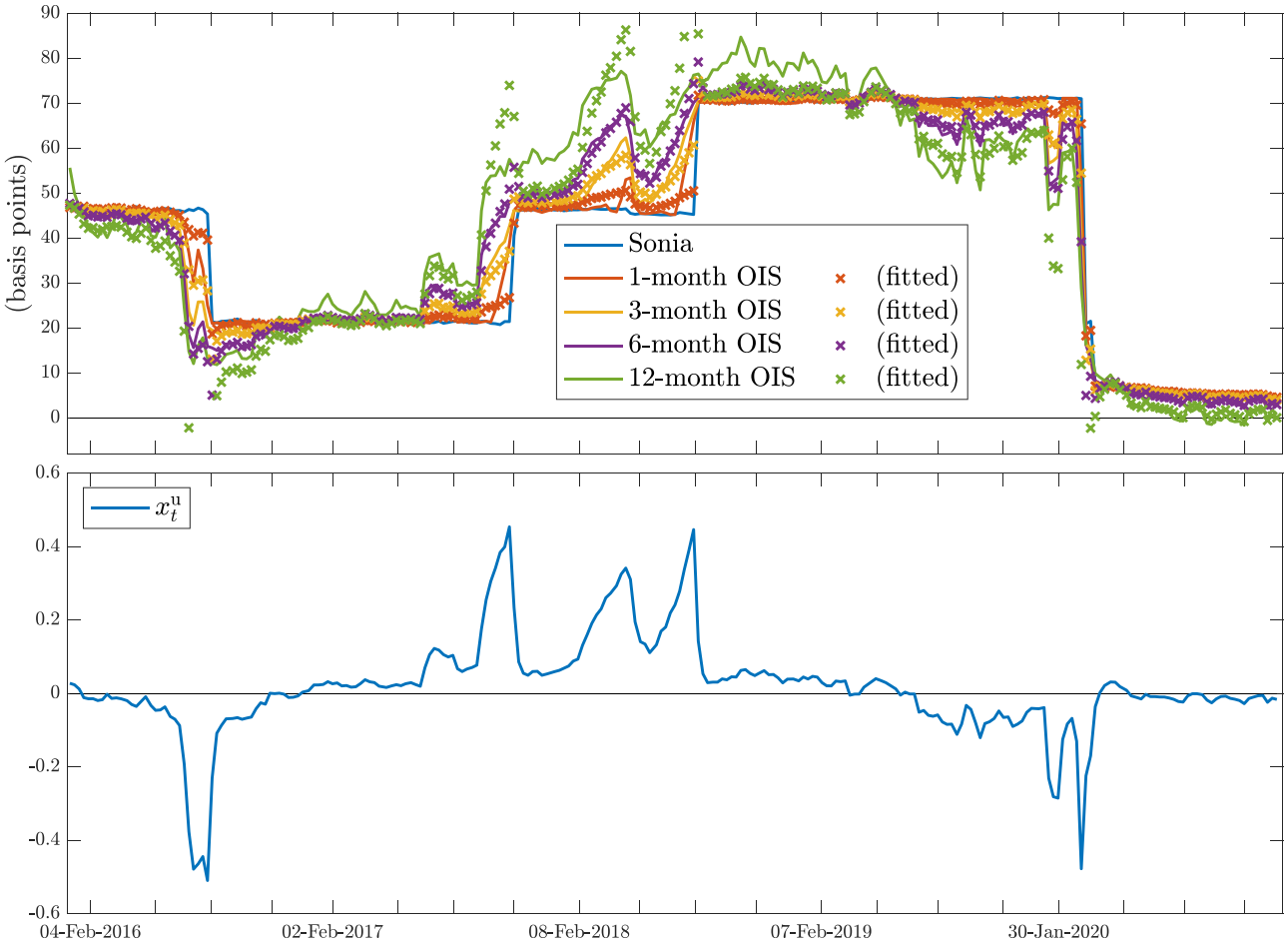

Fig. C2. A comparison of market and model-implied OIS rates in the upper panel, and filtered state variable paths in the lower panel, for an alternative implementation of the model which has only expected jumps.

Table C2
Quasi-maximum likelihood parameter estimates for two implementations of the model: one with only an expected jumps component and a second with only an unexpected jumps component. Both include asymptotic standard errors in parentheses.

Model		Expected-jumps-only model	Unexpected-jumps-only model
State variable		x_t^{e}	x_t^{u}
Superscript		e	u
Model parameters	κ	-	0.5723
			(0.0095)
	θ	-	-0.1071
			(0.0033)
	σ	0.2741	0.2764
		(0.0194)	(0.0020)
	β	0.3069	-
		(0.1512)	
	μ	-0.4570	-0.9779
		(0.3201)	(0.0234)
$\sigma_{\text{error}} \times 10^4$		1.4448	2.3861
Log-likelihood $\times 10^{-3}$		4.3377	4.0739

Appendix D. Adding a spike component

One could generalise (3) with a spikes term:

$$dr_t^* = J_t^{\mathrm{e}}\, dN_t^{\mathrm{e}} + J_t^{\mathrm{u}}\, dN_t^{\mathrm{u}} + dS_t, \tag{D1}$$

where S_t is a spike process; for example, in line with Andersen and Bang (2020), one could specify

$$dS_t = -\kappa S_t\, dt + J_t^{\mathrm{s}}\, dN_t^{\mathrm{e}},$$

where J_t^{s} is the spike size arriving at the expected jump times, and κ governs the rate at which spikes decay. Unexpected spikes could also be included.

For a simple illustration, we let $J_t^{\mathrm{s}} = x_t^{\mathrm{s}}$, where x_t^{s} is an auxiliary state variable like those in Section 2.3:

$$dx_t^{\mathrm{s}} = \kappa^{\mathrm{s}}(\theta^{\mathrm{s}} - x_t^{\mathrm{s}})\, dt + \sigma^{\mathrm{s}}\, dW_t^{\mathrm{s}},$$

for a standard Brownian motion W_t^{s}.

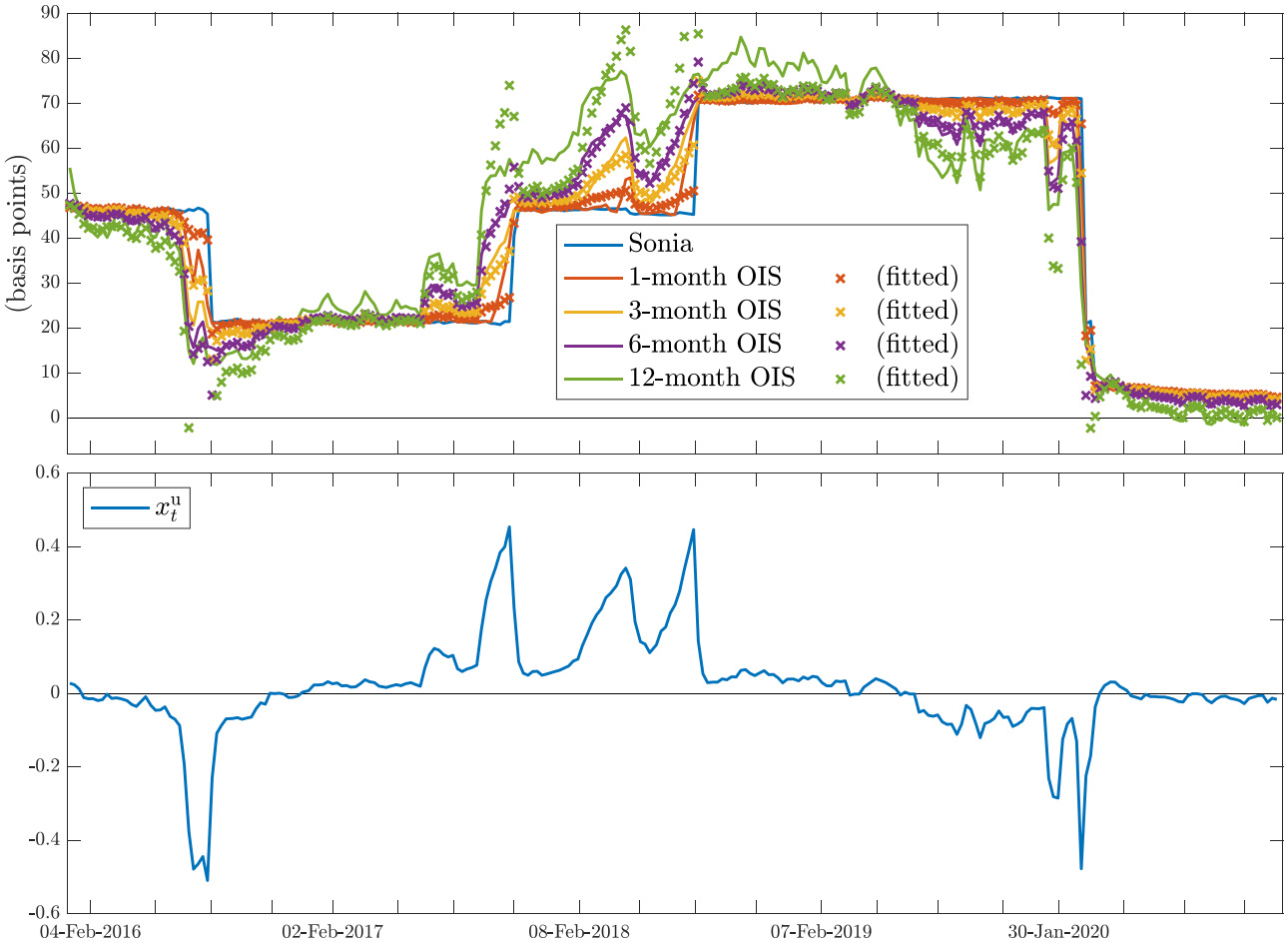

Fig. C3. A comparison of market and model-implied OIS rates in the upper panel, and filtered state variable paths in the lower panel, for an alternative implementation of the model has only unexpected jumps.

Taking the spikes component to be independent of other aspects of the model, we numerically implement the generalised model (D1) as per Section 3.3; in particular, we compute the quantity $\mathbb{E}_t\left[e^{-\int_t^T S_u du}\right]$, which allows us to add artificial spikes to our Sonia and OIS data (via (11) and (12)). We set $\kappa = 30$ (to ensure a realistic, roughly one-day decay of the initial spike), $\kappa^s = 0.6$ (to ensure a significant reversion to θ^s), $\sigma^s = 2\%$ (to allow for stochastic variation in the spike magnitude), and consider various values of θ^s—two, five and ten bps—to obtain average spikes of various magnitudes. Ten basis-point spikes would be considered relatively minor in many contexts (e.g., SOFR), but would nevertheless cause problems for our model (and would necessitate the generalised model in this section).

To see this, we estimate our (non-generalised) model on artificially spiked Sonia and OIS data. Fig. D.1 shows the resultant fit and state variable paths, with the upper two panels corresponding to the $\theta^s = 2$bps case (where spikes are two bps on average) and the lower panels corresponding to $\theta^s = 10$bps. Even in the latter case, the effect on OIS rates is minor (see Footnote [8]). However, the model fit is severely disturbed by the spikes. This is because the non-generalised model fails to recognise spikes, i.e., it prices term rates on the assumption that a spiked Sonia value will persist. This leads to unstable state variable values around spike times—with the model attempting to match term rates without correctly recognising the spike—and altered parameter estimates.

Appendix E. Option pricing

For a given caplet, the at-the-money strike is fair swaplet rate, for the swaplet corresponding to the caplet. Let K^L_{tTS} denote this rate at time t, for a swaplet or caplet linked to the interbank rate L_{TS}, we have

$$\mathbb{E}_t\left[e^{-\int_t^S r_u^* du}(L_{TS} - K^L_{tTS})\right] = 0.$$

This ensures that the at-the-money caplet and floorlet have an equal value, as

$$\mathbb{E}_t\left[e^{-\int_t^S r_u^* du}(L_{TS} - K^L_{tTS})^+\right] - \mathbb{E}_t\left[e^{-\int_t^S r_u^* du}(K^L_{tTS} - L_{TS})^+\right]$$

$$= \mathbb{E}_t\left[e^{-\int_t^S r_u^* du}(L_{TS} - K^L_{tTS})\right].$$

Therefore,

$$K^L_{tTS} = \frac{\mathbb{E}_t\left[e^{-\int_t^S r_u^* du} L_{TS}\right]}{\mathbb{E}_t\left[e^{-\int_t^S r_u^* du}\right]} = \frac{P^*_{tT}/\mathbb{E}_t\left[e^{-\int_T^S \lambda_u^{(T)} du}\right] - P^*_{tS}}{P^*_{tS}(S-T)}, \tag{E.1}$$

where the final line applies some iterated-conditioning manipulations to express the quantity in terms of our model variables. This can be computed with the finite-difference methods described in Appendix B.1, but with one addition scheme with a non-zero

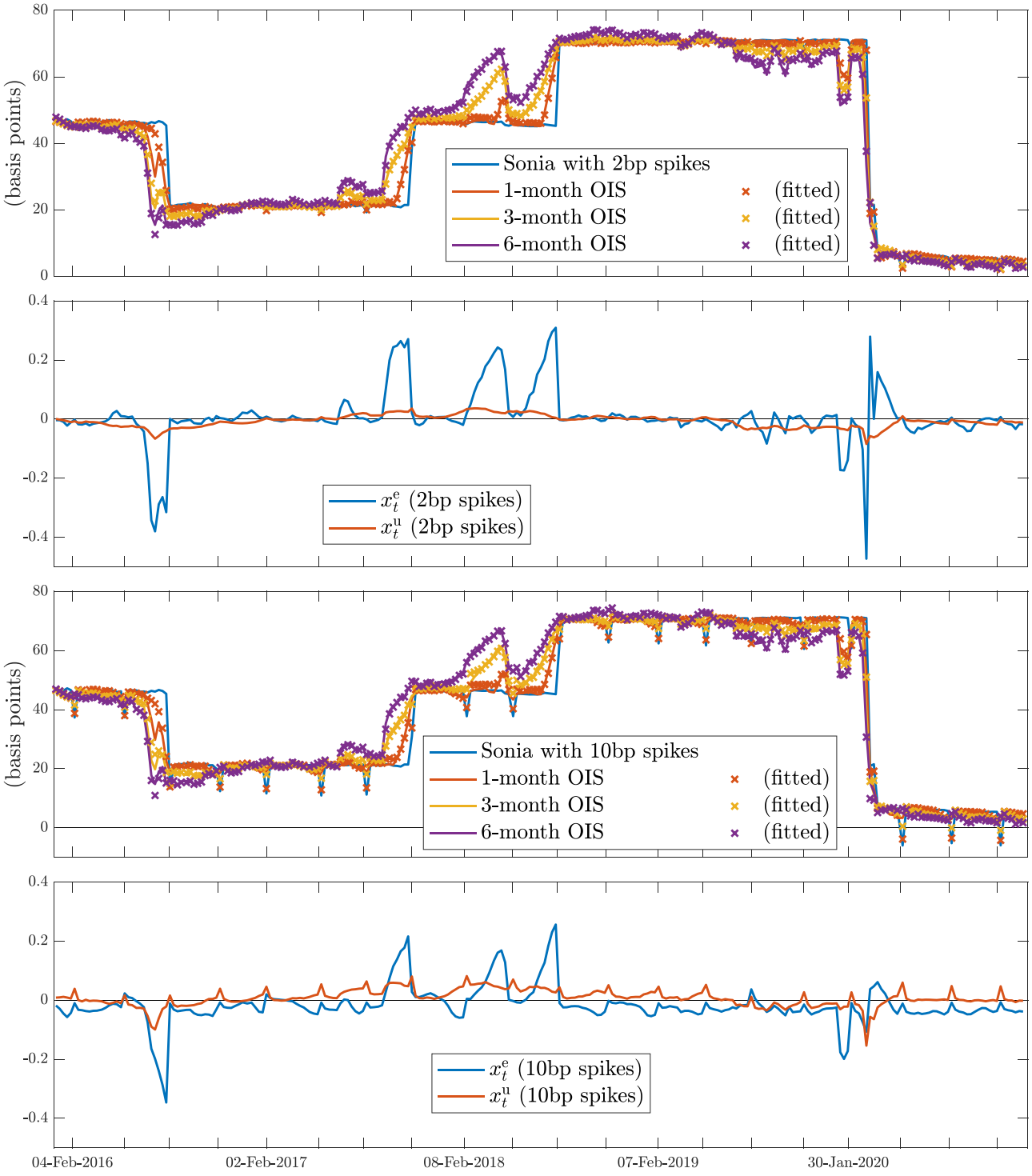

Fig. D1. The first and third panel show comparisons of artificially spiked OIS data and model-fitted OIS rates. The spikes have an average of two and ten bps, respectively. The second and fourth panels show, respectively, filtered state variable paths for these two cases.

terminal condition $\mathbb{E}_T\left[e^{-\int_T^S \lambda_u^{(T)} du}\right]$. Monte Carlo can also be used, especially if the caplet is being priced in this way, because the common random numbers between the strike estimate and the caplet-price estimate reduces sampling error.

The downgrade term $\mathbb{E}_t[e^{-\int_T^S \lambda_u^{(T)} du}]$ would not appear if the caplet were OIS linked, or backward-looking. Letting K^B_{tTS} denote the at-the-money strike of a backward-looking version of the caplet considered above, one obtains the following from the same argument:

$$K^B_{tTS} = \frac{\mathbb{E}_t\left[e^{-\int_t^S r_u^* du} B_{TS}\right]}{\mathbb{E}_t\left[e^{-\int_t^S r_u^* du}\right]} = \frac{P^*_{tT} - P^*_{tS}}{P^*_{tS}(S-T)}. \tag{E.2}$$

Fig. E.1 shows caplet prices implied by our estimated model, as in Fig. 5 but with different accrual structures. The top panel shows forward- and backward-looking caplets, corresponding to (24) and

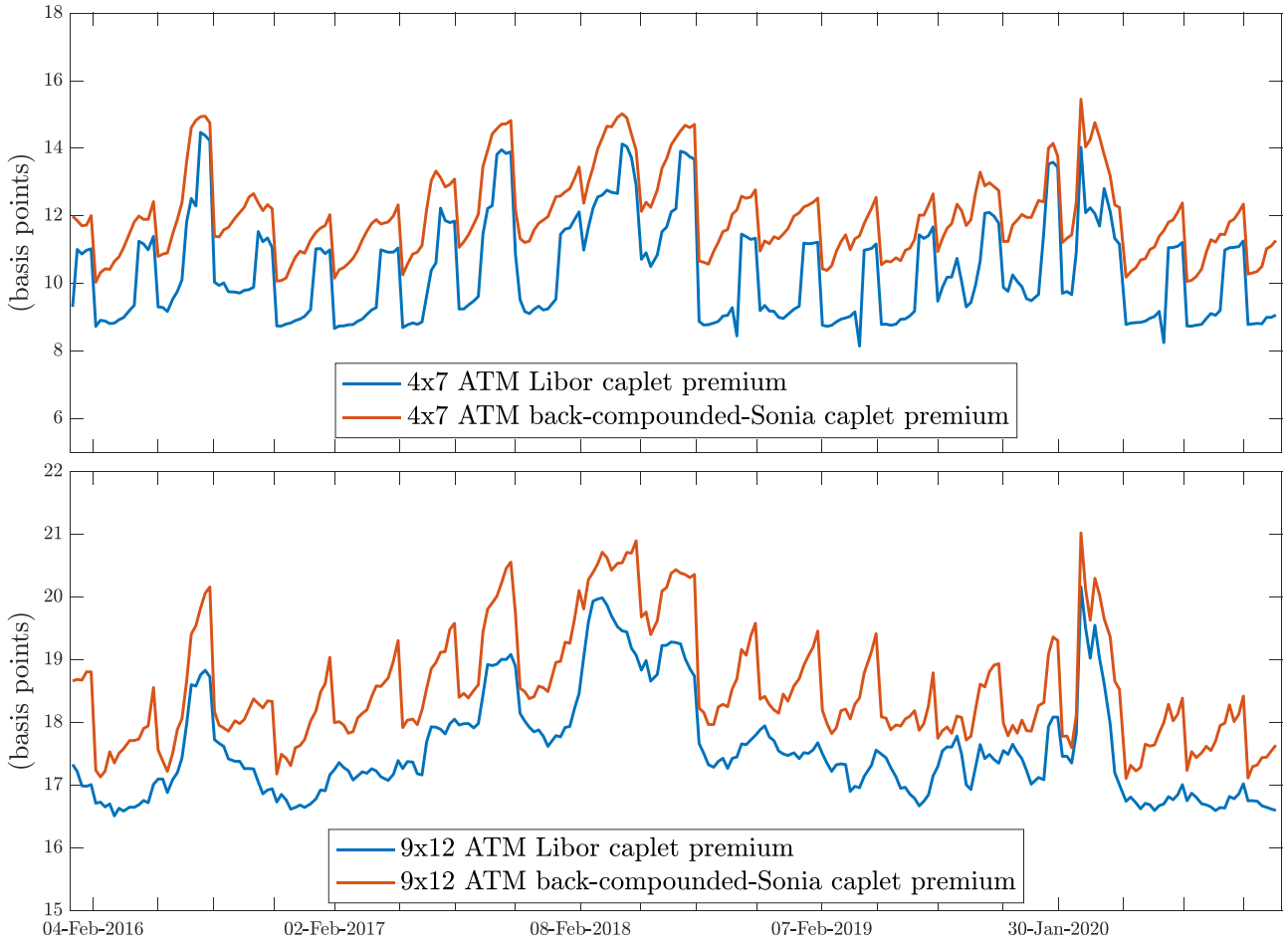

Fig. E1. A comparison of at-the-money (ATM) caplet premia. The upper panel considers caplets with four months until the three-month underlying accrual period starts; the lower panel considers caplets with nine months until the same three-month accrual.

Table E1
The term structure of at-the-money (ATM) swaption-implied volatilities implied by our fitted model, on average over our sample, expressed in basis points. Option expiries range from one month (1m) to twelve months (12m), while the underlying is a one-year swap with quarterly fixed-for-floating payments.

	Implied volatility				
	1m	2m	3m	6m	12m
ATM OIS Swaption	34.23	40.01	43.91	49.53	54.26
ATM Libor Swaption	34.28	40.08	43.97	49.57	54.29

(25), with $T = \frac{4}{12}$ and $S = \frac{7}{12}$, i.e., '4x7' caplets. The forward-looking caplet becomes time inhomogeneous, as there are occasionally two jump times applicable before the reference rate is realised in four months' time. The premium drops when a jump time is passed, and only one relevant jump time remains. The bottom panels shows a '9x12' caplet, i.e., (24) and (25) with $T = \frac{9}{12}$ and $S = 1$. The forward-looking caplet is largely time homogeneous, with a constant three expected jump times in the relevant period of the option. As mentioned in Section 3.5, the time inhomogeneity of the forward-looking caplet is less pronounced, as the passing of one jump time has less relative significance; option premia drop by just under 10% upon a jump time.

Table E.9 shows the implied volatility term structure exhibited by our fitted model, on average throughout the sample. We calculate at-the-money swaption values implied by our model with

$$\mathbb{E}_t\left[\left(\sum_{i=1}^{4} e^{-\int_t^{\tau+i/4} r_u^* du}(0.25)(K^L_{\tau,\tau+(i-1)/4,\tau+i/4} - K)\right)^+\right],$$

where the option-expiry τ ranges from one to twelve months, and where K is set each week (the at-the-money strike sets the value of the forward-starting swap, i.e. the value above excluding the positive-part function, to zero). The forward rates $K^L_{\tau,\tau+(i-1)/4,\tau+i/4}$, prevailing at time τ pertaining to the accrual periods of the underlying swap, are given in (E.1). If the underlying swap is linked to the three-month OIS rate, rather than three-month Libor, the forward rates must be replaced by $K^B_{\tau,\tau+(i-1)/4,\tau+i/4}$ as in (E.2). We then imply a Bachelier, or Gaussian, volatility, using the standard formula with OIS discounting (see, e.g., Filipović et al. (2017, §4.A). Like the time-series volatilities in Table 4, an increasing term structure is exhibited; like in Fig. 5, volatilities are in the region of 35 to 60bps (note that the time-series volatilities in Table 4 are not annualised).

References

Alfeus, M., Grasselli, M., Schlögl, E., 2020. A consistent stochastic model of the term structure of interest rates for multiple tenors. Journal of Economic Dynamics and Control 114, 103861.
Andersen, L.B., Bang, D.R., 2020. Spike modeling for interest rate derivatives with an application to SOFR caplets. Available at SSRN 3700446.
Babbs, S.H., Webber, N., 1994. A theory of the term structure with an official short rate. Financial Options Research Centre Working Paper, University of Warwick (94/49).
Backwell, A., Macrina, A., Schlögl, E., Skovmand, D., 2019. Term rates, multicurve term structures and overnight rate benchmarks: A roll-over risk approach. Available at SSRN 3399680.
Bank of England,. https://www.bankofengland.co.uk/monetary-policy. Accessed in June 2021.
Björk, T., 2004. Arbitrage Theory in Continuous Time. Oxford University Press.

Brigo, D., Mercurio, F., 2001. A deterministic–shift extension of analytically–tractable and time–homogeneous short–rate models. Finance and Stochastics 5 (3), 369–387.
Brigo, D., Mercurio, F., 2007. Interest Rate Models – Theory and Practice: With Smile, Inflation and Credit. Springer Science & Business Media.
Christoffersen, P., Dorion, C., Jacobs, K., Karoui, L., 2014. Nonlinear Kalman filtering in affine term structure models. Management Science 60 (9), 2248–2268.
Crepey, S., 2013. Financial Modeling: A Backward Stochastic Differential Equations Perspective. Springer.
Duffie, D., Singleton, K.J., 1999. Modeling term structures of defaultable bonds. Review of Financial Studies 12 (4), 687–720.
Dybvig, P.H., Ingersoll Jr, J.E., Ross, S.A., 1996. Long forward and zero-coupon rates can never fall. Journal of Business 1–25.
Filipovic, D., 2009. Term-Structure Models: A Graduate Course. Springer.
Filipović, D., Larsson, M., Trolle, A.B., 2017. Linear-rational term structure models. Journal of Finance 72 (2), 655–704.
Filipović, D., Trolle, A.B., 2013. The term structure of interbank risk. Journal of Financial Economics 109 (3), 707–733.
Fontana, C., Grbac, Z., Gümbel, S., Schmidt, T., 2020. Term structure modelling for multiple curves with stochastic discontinuities. Finance and Stochastics 1–47.
Gellert, K., Schlögl, E., 2021. Short rate dynamics: a Fed Funds and SOFR perspective. FIRN Research Paper Forthcoming.
Heath, D., Jarrow, R., Morton, A., 1992. Bond pricing and the term structure of interest rates: A new methodology for contingent claims valuation. Econometrica: Journal of the Econometric Society 77–105.
Henrard, M., 2007. The irony in the derivatives discounting. Wilmott Magazine 3, 92–98.
Jiao, Y., Ma, C., Scotti, S., 2017. Alpha-CIR model with branching processes in sovereign interest rate modeling. Finance and Stochastics 21 (3), 789–813.
Kim, D.H., Wright, J.H., 2014. Jumps in bond yields at known times. Technical Report. National Bureau of Economic Research.
Klingler, S., Syrstad, O., 2021. Life after LIBOR. Journal of Financial Economics 141 (2), 783–801.
Lyashenko, A., Mercurio, F., 2019. Looking forward to backward-looking rates: a modeling framework for term rates replacing LIBOR. Available at SSRN 3330240.
Newey, W.K., West, K.D., 1987. A simple, positive semi-definite, heteroskedasticity and autocorrelation consistent covariance matrix. Econometrica 55 (3), 703–708.
Piazzesi, M., 2001. An econometric model of the yield curve with macroeconomic jump effects. Technical Report. National Bureau of Economic Research.
Piazzesi, M., 2010. Affine term structure models. In: Handbook of Financial Econometrics: Tools and Techniques. Elsevier, pp. 691–766.
Piterbarg, V., 2020. Interest rates benchmark reform and options markets. Available at SSRN 3537925.
Schrimpf, A., Sushko, V., 2019. Beyond LIBOR: a primer on the new reference rates. BIS Quarterly Review.
Shreve, S.E., 2004. Stochastic Calculus for Finance II: Continuous-time Models, Vol. 11. Springer Science & Business Media.
Skov, J.B., Skovmand, D., 2021. Dynamic term structure models for SOFR futures. Journal of Futures Markets 41 (10), 1520–1544.
Trolle, A.B., Schwartz, E.S., 2009. A general stochastic volatility model for the pricing of interest rate derivatives. Review of Financial Studies 22 (5), 2007–2057.